EXPLORING CAPILLARY ELECTROPHORESIS METHODS FOR THE AFFINITY
INTERACTION OF INDOLICIDIN AND LIPOPOLYSACCHARIDE

by

Erika Dufort-Lefrancois

B.Sc., Royal Roads University, 2007

A THESIS SUBMITTED IN PARTIAL FULFILLMENT OF THE REQUIREMENTS
FOR THE DEGREE OF
MASTER OF SCIENCE IN ENVIRONMENTAL SCIENCES

in

The Faculty of Graduate Studies
(Master of Environmental Science, *Chemistry*)

Thesis examining committee:

Heidi Huttunen-Hennelly (PhD), Associate Professor and Thesis Supervisor,
Department of Physical Sciences (Chemistry)

Jonathan Van Hamme (PhD), Associate Professor and Committee Member,
Department of Biological Sciences

Mark Paetkau (PhD), Associate Professor and Committee Member,
Department of Physical Sciences (Physics)

Jeffrey Guthrie (PhD), Assistant Professor and External Examiner, Eastern Michigan
University, Department of Chemistry

April 2015

Thompson Rivers University

Thesis Supervisor: Associate Professor Heidi Huttunen-Hennelly

ABSTRACT

Indolicidin (indol) is a cationic antimicrobial peptide that is isolated from the cytoplasmic granules of bovine neutrophils. Known primarily for its high percentage of tryptophan residues, indol is of particular interest due to its broad spectrum of antimicrobial activity. While there is currently a lot of information available on the minimum inhibitory concentration for indol, as well as for its overall spectrum of activity, there remains a gap in knowledge about the mechanism of action and a binding constant (K_b) has not yet been reported for its interaction with its proposed receptor- lipopolysaccharide (LPS).   This thesis focuses on investigating capillary electrophoresis (CE) methods for studying the interaction of indol with LPS at physiological pH with the ultimate goal of generating a K_b.

In Chapter 2, the effect of incubation time is explored using pre-incubation CE. The findings indicate a slow equilibrium that is established at upwards of six hours. K_b values of decreasing magnitude are generated at 2, 5.5 and 10 h ($\pm$ 0.5) incubation times, each data set indicated that formation of the complex is favoured and multiple binding stoichiometries are likely present.

Chapter 3 outlines optimized affinity CE parameters with indol as a constant concentration sample and LPS added to the background electrolyte. A molecular mass range is assumed for LPS to produce a conservative K_b range for the interaction of indol and LPS. The results agreed with those of Chapter 2, suggesting multiple binding sites and that complex formation is favoured. Finally, attempted use of the frontal analysis CE (FACE) method is described in Chapter 4, outlining

optimized parameters and suggestions for successful use of the FACE method. Combined, Chapters 2, 3 and 4 set the groundwork for a confident K_b to be reported for the interaction of indol with LPS. Additionally, those methods will translate nicely to the study of indol or its derivatives with mammalian cells in future work.

TABLE OF CONTENTS

ACKNOWLEDGEMENTS

I would like to express my heartfelt gratitude to my wonderful supervisor, Dr. Heidi Huttunen-Hennelly, whose incredible guidance and support was matched by her intelligence and humility. You continue to inspire me both personally and academically. I am also grateful to Dr. Kingsley Donkor for his dedicated time and patience.

To my committee members, Dr. John Van Hamme and Dr. Mark Paetkau, and to my external examiner, Dr. Jeff Guthrie, thank you for your dedicated time to reading my thesis and your contributions to its improvement.

Thank you very sincerely to Laiel Soliman, without your friendship, advice, guidance and support, this experience would have been wholly different. I hope to someday be as helpful to someone as you have been to me.

I would like to acknowledge the Internal Research Fund for Scholarship and Scholarly Teaching as well as the Environmental Science and Natural Resource Science Fellowship Award from Thompson Rivers University for their financial assistance with this project.

Lastly, where would I be without the caring support of my family? Thank you for constantly believing in me.

DEDICATION

À mon bien-aimé, je t'aime de tout mon coeur.

LIST OF FIGURES AND REACTIONS

LIST OF TABLES

LIST OF IMPORTANT TERMS AND ABBREVIATIONS

ACE	Affinity capillary electrophoresis
AMP	Antimicrobial peptide
BGE	Background electrolyte
CAP	Cationic antimicrobial peptide
CE	Capillary electrophoresis
CMC	Critical micelle concentration
D	Drug
DCM	Dichloromethane
DMF	Dimethylformamide
DMSO	Dimethyl sulfoxide, neutral marker
DP	Drug-protein complex
EOF	Electroosmotic flow
FACE or FA	Frontal analysis capillary electrophoresis
g	Grams
H	Hours
HCTU	2 - (6 - Chloro - 1H - benzotriazole - 1 - yl) - 1,1,3,3 - tetramethylaminium hexafluorophosphate (Activating agent)
HD	Hummel-dreyer method
HPLC	High pressure liquid chromatography

Indol	Indolicidin
L	Litres
LPS	Lipopolysaccharide
L_t and L_d	Total capillary length and capillary length to detector
K or K_b	Equilibrium constant, also termed binding constant
min	Minutes
mol	Moles
NMM	N-methyl morpholine
P	Protein
PI-ACE	Pre-incubation affinity capillary electrophoresis
ppm	Parts per million, $mg \cdot L^{-1}$ equivalent
R^2	linear correlation coefficient
s	Seconds
SPPS	Solid phase peptide synthesis
TFA	Trifluoroacetic acid
μ	electrophoretic mobility
v/v	volume per volume
WPW motif	Tryptophan-Proline-Tryptophan in a peptide sequence

CHAPTER 1: INTRODUCTION

The constant overuse and misuse of antibiotics, especially with livestock, has accelerated the emergence of antibiotic resistant bacteria and has made the search for alternative treatments much more urgent (1). The search for new viable drugs has been extensive for many decades with natural products being at the forefront of the drug discovery and development process (2). Combinatorial libraries, which became popular in the 1990s, did not yield the expected surge in productivity and focus has returned to research with a basis in natural products. Research surrounding drug receptors and binding is important for drug advancement. The information about indolicidin (indol), lipopolysaccharide (LPS) and capillary electrophoresis (CE) to follow is not meant to be exhaustive, but should provide some insight for readers whose expertise lie elsewhere.

Indolicidin

From the search for alternative therapeutic agents came a family of drugs known as antimicrobial peptides (AMPs). Many living organisms, including plants, animals, bacteria and fungi, produce AMPs for defense against invading pathogens (3). They employ multiple modes of action against their targets, making them effective against many pathogen strains and render them less likely to themselves become drugs to which microbes develop resistance (4). Small, cationic amphiphilic peptides are being studied as a novel class of antimicrobials and those used as topical antibiotics have progressed to phase III of clinical trials (5). Indolicidin (indol) is a cationic AMP that is isolated from bovine neutrophils (6). It has antibiotic properties against

Gram-positive and Gram-negative bacteria, and exhibits activity against protozoa, HIV, fungi, and neoplastic cells (6-8). Indol is composed of 13 amino acids, is one of the shortest known naturally-occurring AMPs and is renowned for its high percentage of tryptophan (38%) and disordered structure (6, 9-11) (Figure 1.1).
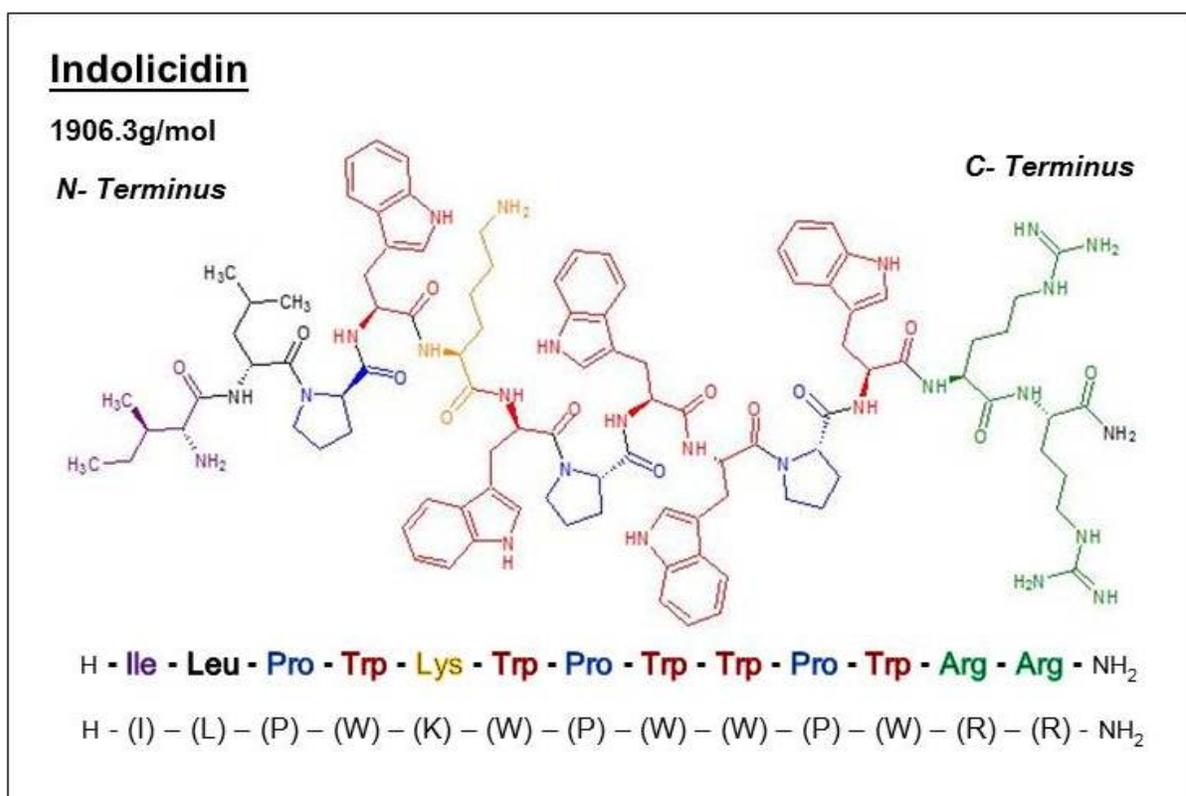
Figure 1.1: Structure for the antimicrobial peptide Indolicidin.

The peptide also has proline and arginine residues which prevent secondary structure from forming and provide the cationic nature, respectively (9, 11). The rich quantity of tryptophan residues and the two WPW (tryptophan, proline, tryptophan) motifs present in the indol structure are thought to be responsible for

much of its antimicrobial activity (10, 12). At physiological pH, indol has a charge of +4 and is thought to enter the cell through defects that it creates in the membrane in addition to several other proposed mechanism briefly described later(6).

Despite its antimicrobial properties, indol is impractical in its current, unaltered form due to its toxicity to both prokaryotes and eukaryotes (10, 12). To overcome this, many mutants of indol have been created that render it less hemolytic while simultaneously increasing its antimicrobial properties (13-15). In one study, by way of solid phase peptide synthesis, five indol derivatives were formed by incrementally substituting the very hydrophobic tryptophans with the mildly hydrophobic alanines (13). For the derivative known as $\Delta45$, only the 4th and 5th tryptophans in the peptide sequence were substituted, allowing one of the WPW motifs to remain intact. This derivative showed the greatest promise. Further research and development of AMPs such as $\Delta45$ could be a step towards a class of drugs that are highly effective against many pathogens, with the prospect of remaining functional over time. Additionally, combination studies blending indol and other therapeutic agents have shown increased antimicrobial action (16).

Much is known about the properties and interactions of indol: It has the ability to cause membrane-thinning by disruption of headgroups, it adopts different equilibrium conformations in solution, and it shows bactericidal action against the typically antibiotic resistant *Pseudomonas aeruginosa*- a ubiquitous, problematic, and opportunistic pathogen (16-18). The precise mechanism of bacterial cell attack is not confirmed, but many have been suggested. They include inhibition of protein and DNA synthesis, cell leakage via channel formation across the membrane, pore and non-pore forming mechanisms among others (17, 19-23). The development of a drug

prospect that attacks only cell membranes would be problematic as it would not possess the specificity required to single out pathogens while leaving human cells intact. It is for this reason that the multiple modes of attack available to AMPs such as indol are of such value. In studies of antibiotic resistance, Gram-negative bacteria are the more abundant source of antibiotic resistance genes and are responsible for more costs and resources in the care of hospital patients (24, 25). It is for this reason that drug research surrounding Gram-negative bacteria often trumps that of its Gram-positive counterpart. An important part of continued research involves a specific study of the interaction of indol with LPS- its proposed corresponding receptor in Gram-negative bacteria (22). Once studies have been conducted between indol and LPS, it is then simply a matter of reproducing similar studies with lipoteichoic acid- the LPS equivalent in Gram-positive bacteria in order to expand the findings to both types of pathogenic bacteria (26).

Lipopolysaccharide

The complex structure of the Gram-negative cell envelope contains LPS in its outer membrane, a component that is absent in the composition of Gram-positive bacteria (Figure 1.2). The role of the outer membrane is to act as a barrier between the cytoplasm of the cell and the environment. LPS, a large component of Gram-negative outer membranes, has the amphipathic properties of phospholipids and serves several functions. Of utmost importance is its role in semi-permeability, only allowing passage of low molecular weight and hydrophilic molecules (27). The LPS structure can be broken into three parts: lipid, core and O-antigen (Figure 1.3) (27, 28). The lipid portion is generally referred to as "lipid A". It consists of a phosphorylated N-acetylglucosamine dimer attached to six or seven saturated fatty

acids. It is hydrophobic and serves to anchor LPS to the membrane. The lipid A portion of the molecule is responsible for LPS's toxic properties (28). The core portion is also known as the "R-polysaccharide" or "core oligosaccharide". The core consists of a chain of sugars. The 2-keto-3-deoxyoctonoic acid is a sugar that is so unique to LPS that it can be used in LPS assays.   Unlike the structure of Lipid A, which is highly conserved among Gram-negative bacteria, the core polysaccharide structure of LPS varies among bacterial genera. Lastly, the O-antigen region is made up of up to 40 repeating 3 - 5 sugar subunits. This portion of the LPS molecule is the biggest, is hydrophilic and the sugars involved are very unique and can even vary within a species (27).
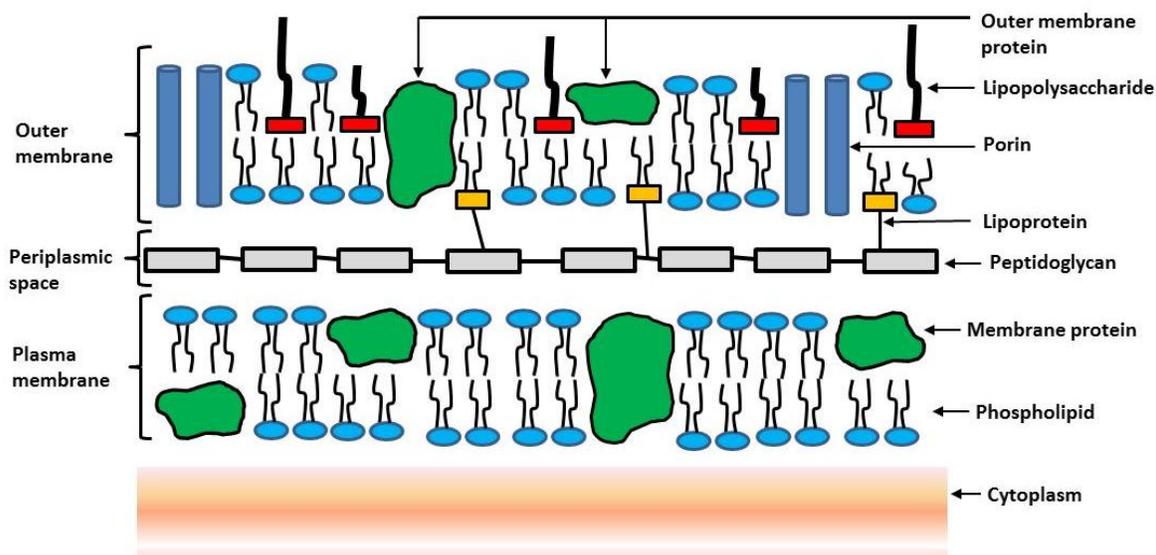
Figure 1.2: Structure of the cell envelope of Gram-negative bacteria. This figure created with guidance from (27).

As previously described, the actual structure of an LPS unit can vary quite substantially from one species to another and even within a species of bacteria. Knowing the precise structure of any commercially acquired sample of LPS is difficult as preparations are heterogeneous. In addition, the LPS units are likely to exist in micellar solution when dissolved in solvent, presenting a further challenge. As a single LPS unit, the mass range is approximated at 10-20 kDa (28). In aggregate form, the average mass can be upwards of 1000-4000 kDa. For Sigma Aldrich LPS from *E. coli* 0111:B4 (used herein), micelles are said to form anytime the sample is dissolved in solvent; thus individual LPS units are unlikely to be present during analyses (29). Further research into the critical micelle concentration (CMC) of LPS has found that for the *E. coli* 0111:B4 strain acquired from Sigma-Aldrich, the CMC is 1.3- 1.6 μM and aggregates of 43- 49 molecules per micelles are formed (30). Using a conservative mass estimate of 10-20 kDa per LPS

unit, that places the aggregate mass range at 430- 980 kDa.
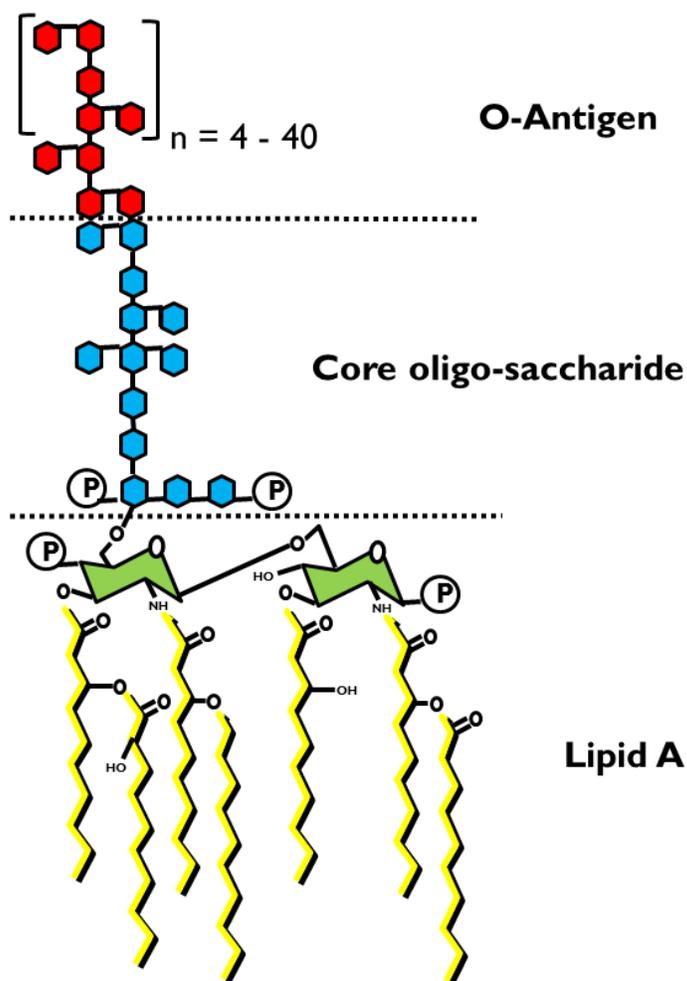
Figure 1.3: General structure of lipopolysaccharide. Reference (26) used to develop this figure.

To study the mechanism of action of indol with LPS, use of intact bacterial cells would be of the greatest benefit for studying the interaction of a prospective drug with its target, however, published studies of this nature are few (5). The

permissions involved and measures required to prevent and mitigate possible biohazards are likely reasons for avoiding their use. Simplifying an interaction study to only include a drug (indol) and one individual receptor (LPS) disregards many important biological features including membrane potential, pH gradients, lipid heterogeneity, and the presence of membrane proteins (5). To reach a broad understanding of interaction mechanisms, it is accepted that the simplified perspective is still helpful. Consequently, once the drug receptor is known, it is used as an analogue to shed light on the interaction. In this particular case, LPS is used to better understand the binding action of indol and its subsequent entry into the cell.

Capillary Electrophoresis

Capillary electrophoresis (CE), also termed High Performance Capillary Electrophoresis (HPCE), encompasses a family of methods for the separation of molecules based on their movement within a small bore capillary (inner diameter of ~25-100μm) under an applied electric field (31). The modes of CE extend to micellar electrokinetic capillary chromatography (MECC), capillary gel electrophoresis (CGE), and capillary isoelectric focusing (CIEF); however, the simple term "CE" usually refers to Capillary Zone Electrophoresis (CZE) whereby separation occurs solely by electrophoretic mobility (32). CE is a young technique when compared to High Performance Liquid Chromatography (HPLC) and Gas Chromatography (GC). In 1967, Hjertén offered a thesis describing an apparatus for free zone electrophoresis in a revolving tube. His thesis was thought to be the direct forerunner of modern CZE (33, 34). The evolution of CE has since flourished and CE related publications have grown exponentially. CE techniques have been applied to

genetics, sequencing of nucleic acids and proteins, studies of diseases, the identification of species and individuals, analysis of complex matrices, separation of very similar molecules (*ie.*, enantiomers and molecules with identical physicochemical properties), binding studies of analytes with ligands, protein conformations and more (11, 33-37). CE is a popular technique due to its high separation efficiency, automation ability, high resolving power, quick analysis time, ability to operate at near physiological pH, and low injection volume resulting in comparatively low operational costs (35, 38).

Binding constants are of great interest in studies of noncovalent molecular interactions (36). The human body alone offers an unlimited number of examples of intricate and complex biological processes. Understanding these processes is aided by the elucidation of a binding constant (K_b), also referred to as an equilibrium constant, which denotes the relationship between a receptor (*R*) and a ligand (*L*), or respectfully, a protein (*P*) and a drug (*D*) (39).

For the equilibrium equation

$$P + D \rightleftharpoons PD \tag{Eq. 1}$$

The relationship of free protein (*P*) and (*D*) to complex (*PD*) can be expressed by the equation where K=K_b *(40)*:

$$K = \frac{[PD]}{[P][D]} \tag{Eq. 2}$$

And the ratio (r) of complexed *P* to total *P* can be expressed as:

$$r = \frac{[PD]}{[P]+[PD]} = \frac{K[D]}{1+K[D]} \qquad \text{(Eq. 3)}$$

When multiple equilibria are considered, a more complex equation is required

(41, 42):

$$\bar{r} = \sum_{i=1}^{i=m} \frac{n_i K_i (D_i)}{1+ K_i (D_i)} \qquad \text{(Eq. 4)}$$

$\bar{r}$ is the mean number of moles of D bound per mole of P,
(D_i) is the free ligand concentration,
n_i is the number of independent sites of class i,
K_i is the association constant with D, and
m is the total number of classes.

In the past, methods such as ultracentrifugation, equilibrium dialysis, radioimmunoassay, nuclear magnetic resonance , fluorescence quenching and slab gel have been used for estimating drug-protein interactions (43). In the last 20 years, CE has become a popular instrument to study the extent of binding and dissociation of formed complexes. Binding studies and the elucidation of a K_b are essential for drug development because pharmacological activity is best correlated to the concentration of unbound drug (36). There are a variety of CE techniques for the study of a K_b that are closely related. These methods can be subdivided by the way the binding parameters are determined. The Affinity CE (ACE), Vacancy Affinity

CE (VACE) and Partial Filling Affinity CE (PFACE) methods measure the change in mobility of the species (44). The Hummel-Dreyer method (HD), Vacancy peak (VP), and Frontal Analysis (FA)/Frontal Analysis Continuous CE (FACCE) methods use peak area or plateau height to determine the K_b. Close inspection of each of these CE methods, coupled with pilot projects of preliminary outcomes have indicated that FACE, ACE and the closely related pre-incubated ACE method, are most suitable for studying the interaction of indol with LPS. These methods are discussed in greater detail.

Affinity Capillary Electrophoresis

ACE is the most commonly used CE technique for the study of protein-drug interactions with roughly 1000 publications on the subject of ACE between 2000-2012 (45, 46). Use of micelles and cyclodextrins, forms of secondary equilibrium, can be considered affinity interactions, however, the term ACE is reserved for studies of noncovalent interactions of biomolecules with different reagents and is at times used as a general term to encompass CE binding studies (33). Capillary wall coatings are commonly used to reduce protein adsorption and improve CE performance (47). Contrarily, it has also been suggested that use of precise rinse protocols can adequately reduce the extent of protein adsorption and produce usable findings with bare fused silica capillaries (48).

The ACE method of studying affinity interaction has the same experimental setup as the HD method. The difference between the methods is in analysis of the resulting electropherogram. While the HD method uses peak area to calculate the equilibrium constant, ACE uses the change in mobility of the injected species (38).

Addition of a neutral marker (e.g. DMSO, mesityl oxide, acetonitrile) serves to indicate the electroosmotic flow (EOF). The calculations of K_b are based on the electrophoretic mobility of free and complexed drug. For an assumed 1:1 binding of *D to P*, the electrophoretic mobility (μ) of *D* is as follows (36, 49):

$$\mu_i = \frac{[D_f]}{[D_f]+[DP]}\mu_f + \frac{[DP]}{[D_f]+[DP]}\mu_c \qquad \text{(Eq. 5)}$$

where μ_i is the apparent electrophoretic mobility of *D*, μ_f is the mobility of free drug (D_f), and μ_c is the mobility of the *DP* complex. Eq. 5 can be rearranged as follows:

$$\frac{[DP]}{[D_f]} = K[P_f] = \left(\frac{\mu_f - \mu_i}{\mu_i - \mu_c}\right) \qquad \text{(Eq. 6)}$$

When employing Eq. (6), μ_c must be determined experimentally but since the small molecular mass of the bound drug is not likely to significantly change the mobility of *P*, it is assumed that $\mu_c \cong \mu_P$ (36). Knowing the true mobility of the complex is almost impossible. From Eqs. 2 and 5, we obtain (36, 49):

$$\mu_i = \frac{\mu_f + \mu_c K[P_f]}{1 + K[P_f]} \qquad \text{(Eq. 7)}$$

$$\left(\mu_i - \mu_f\right) = \frac{(\mu_c - \mu_f)K[P_f]}{1 + K[P_f]} \qquad \text{(Eq. 8)}$$

Further rearrangement of Eq. 8 results in:

$$\frac{1}{(\mu_i - \mu_f)} = \frac{1}{(\mu_c - \mu_f)K} \frac{1}{[P_f]} + \frac{1}{(\mu_c - \mu_f)} \qquad \text{(Eq. 9)}$$

$$\frac{[P_f]}{(\mu_i - \mu_f)} = \frac{1}{(\mu_c - \mu_f)} [P_f] + \frac{1}{(\mu_c - \mu_f)K} \qquad \text{(Eq. 10)}$$

$$\frac{(\mu_i - \mu_f)}{[P_f]} = -K(\mu_i - \mu_f) + K(\mu_c - \mu_f) \qquad \text{(Eq. 11)}$$

The ACE experimental design requires monitoring the change of the migration time for the complexed species (t_c) compared with the marker (t_m) which indicates a change in the electrophoretic mobility (μ_i) of the complex (44). Voltage (V) used, total capillary length (L_t), and the effective length of the capillary (to the detector) (L_d) are also important parameters for the determination of μ_i as follows:

$$\mu_i = \left[\frac{L_t L_d}{V} \right] \left(\frac{1}{t} - \frac{1}{t_m} \right) \qquad \text{(Eq. 12)}$$

The presence of additive in the background electrolyte (BGE) can introduce differences in viscosity as increasing concentrations are added (50). A correction can be made to Eq. 12 to account for the viscosity effect. The effective electrophoretic mobility μ_{eff} is multiplied by the ratio (I_o/I), where I_o is the current without any additives in the buffer solution and I is the current when there is additive in the buffer solution. The corrected μ_{eff} are then used to determine K_b based on the plotting forms shown in Table 1.1.

Each of the plotting methods listed in Table 1.1 best depicts interactions with a 1:1 stoichiometry and linearity of those plots helps to support the assumption of 1:1 binding. Where multiple binding sites are present, non-linearity is best indicated by the X-reciprocal plot (36). Complicated stoichiometries can sometimes be determined by identifying more than one trend on an X-reciprocal plot (51, 52). Elucidation of the correct stoichiometries may require use of different instrumentation (e.g. NMR, UV spectra and MS) (36, 46).

Table 1.1: Plotting forms of binding constant (K_b).

Method (synonymous names)	Plotting Equation (y axis vs x axis)	Determination of K_b	Equation
Nonlinear regression (mobility ratio difference)	$\dfrac{\mu_f-\mu_i}{\mu_i-\mu_c}$ vs $[P_f]$	*slope*	(6)
X-Reciprocal (Eadie plot, Scatchard plot)	$\dfrac{(\mu_i-\mu_f)}{[P_f]}$ vs $(\mu_i-\mu_f)$	*-slope*	(11)
Y-Reciprocal	$\dfrac{[P_f]}{(\mu_i-\mu_f)}$ vs $[P_f]$	$\dfrac{slope}{intercept}$	(10)
Double-reciprocal (Lineweaver–Burk plot, Benesi–Hildebrand plot)	$\dfrac{1}{(\mu_i-\mu_f)}$ vs $\dfrac{1}{[P_f]}$	$\dfrac{intercept}{slope}$	(9)

μ_f, μ_c and μ_i are final/free drug, *DP* complex and apparent electrophoretic mobilities, respectively. $[P_f]$ is the free protein concentration. Table compiled from (36, 49, 53).

From a generated plot, the resulting K_b value is typically given in (L·mol^{-1}) (54-56). In some cases where the molecular mass of the protein or drug is not precisely known, the K_b is at times represented in (g/mL)$^{-1}$, however this notation makes it very difficult to compare and assess relative binding strength (57). In cases where the binding kinetics are deemed to be slow, a modified ACE protocol whereby the drug and the protein are pre-incubated prior to CE analysis is appropriate (58).

Pre-incubation Affinity Capillary Electrophoresis (PI-ACE)

The experimental design of the PI-ACE method is almost identical to that of ACE,

and the treatment of the resulting data is the same. Rather than the addition of one component to the BGE, both the *P* and the *D* are pre-incubated for a set amount of time before CE analysis. A viscosity correction (I_o/I) that accounts for the change in current due to change in BGE is not needed because run buffer and thus current remains unchanged. The μ_{eff} simply becomes μ_c -μ_f and all the same plotting forms depicted in Table 1.1 apply. The PI-ACE method is of interest for the investigation of the indol-LPS binding because it is well suited for studying slow binding kinetics. In preliminary investigations of the indol-LPS interaction, slow establishment of the equilibrium is indicated (described in Chapter 2). One additional parameter that must be monitored is the amount of time that the samples are incubated prior to introduction to the CE instrument. Either the *P* or *D* (LPS or indol) can be varied in the pre-incubated samples.

Frontal Analysis Capillary Electrophoresis (FACE)

The greatest benefit of the FACE experimental design for determining a K_b is that it does not require the assumption of a 1:1 binding stoichiometry (59). FACE is also known to be a robust, simple, and reliable method for the determination of a K_b (44, 60). Injection of large "plugs" of sample for 1-2 mins results in a plateau rather than the usual peaks that are produced from short 1-5 second injections. As with any other CE methods, experimental parameters (ie. buffer type and concentration, voltage, injection time, etc) are first optimized. For this method to be successful, the mobility of the drug must differ sufficiently from the mobility of the complex/protein (44).   For K_b determination, pre-incubated samples of increasing concentration of drug and constant concentration of protein are injected together.

Prior to analysis of pre-incubated samples, a calibration curve of free drug plateaus of increasing height is built that will be used to quantify the fraction of free drug (61). In the pre-incubated samples, the free drug will migrate at a different rate than the complex and emerge later in the electropherogram, allowing determination of the fraction of free drug when plateau heights are compared to the calibration. This data is used to plot the number of complexed molecules per molecule of protein as a function of the free drug concentration (62). The resulting binding curve is fit using non-linear regression.

Research Objectives

The primary objective of this thesis is to explore the indol-LPS interaction and determine the most suitable CE method to elucidate a K_b at physiological pH. A secondary objective is to report a preliminary K_b for the indol-LPS binding equilibrium. A K_b value will shed light on the strength of the binding between indol and LPS, corroborate the assumption that LPS is the primary receptor for indol, and represent a first step to determining the precise type of non-covalent interaction present. Successes and failures of PI-ACE, ACE, and FACE attempts are presented in Chapters 2, 3 and 4, respectively. They represent a veritable roadmap for use of CE for the study of indol's interactions with LPS. From the optimized CE parameters outlined in this thesis, further studies of indol and its derivatives with other bacterial or mammalian cell wall components can continue to broaden our understanding of this unique AMP.

References

1. Levy S. Reduced antibiotic use in livestock: how Denmark tackled resistance. Environ Health Perspect. 2014 Jun;122(6):A160-5.

2. Newman DJ, Cragg GM. Natural products as sources of new drugs over the 30 years from 1981 to 2010. J Nat Prod. 2012 Mar 23;75(3):311-35.

3. Reddy KVR, Yedery RD, Aranha C. Antimicrobial peptides: premises and promises. Int J Antimicrob Agents. 2004 12/01;24(6):536-47.

4. Peschel A, Sahl H. The co-evolution of host cationic antimicrobial peptides and microbial resistance. Nat Rev Microbiol. 2006 07;4(7):529-36.

5. Hancock REW, Rozek A. Role of membranes in the activities of antimicrobial cationic peptides. FEMS Microbiol Lett. 2002;206(2):143-9.

6. Selsted ME, Novotnytll MJ, Morris WL, Tang Y, Smith W, Cullor JS. Indolicidin, a Novel Bactericidal Tridecapeptide Amide from Neutrophils. J Biol Chem. 1991;267(7):4292-5.

7. Ahmad I, Perkins WR, Lupan DM, Selsted ME, Janoff AS. Liposomal entrapment of the neutrophil-derived peptide indolicidin endows it with in vivo antifungal activity. Biochim Biophys Acta. 1995 7/26;1237(2):109-14.

8. Aley SB, Zimmerman M, Hetsko M, Selsted ME, Gillin FD. Infect Immun. 1994(62):5397-5403.

9. Andreu D, García F. An optimized Boc synthesis of indolicidin. Lett Pept Sci. 1997;4:41.

10. Bowdish DM, Davidson DJ, Scott MG, Hancock RE. Immunomodulatory activities of small host defense peptides. Antimicrob Agents Ch. 2005 May;49(5):1727-32.

11. Jones DS, Huttunen-Hennelly HE, Donkor KK. The design and synthesis of alanine-based indolicidin derivatives with identical physicochemical properties and their separation using capillary electrophoresis. Anal Bioanal Chem. 2010 Dec;398(7-8):3073-9.

12. Falla TJ, Karunaratne DN, Hancock REW. Mode of Action of the Antimicrobial Peptide Indolicidin. J Biol Chem. 1996 08;271(32):19298-303.

13. Podorieszach AP, Huttunen-Hennelly H. The effects of tryptophan and hydrophobicity on the structure and bioactivity of novel indolicidin derivatives with promising pharmaceutical potential. Org Biomol Chem. 2010 04;8(7):1679-87.

14. Bhargava A, Osusky M, Hancock RE, Forward BS, Kay WW, Misra S. Antiviral indolicidin variant peptides: Evaluation for broad-spectrum disease resistance in transgenic Nicotiana tabacum. Plant Sci. 2007 3;172(3):515-23.

15. Sader HS, Fedler KA, Rennie RP, Stevens S, Jones RN. Omiganan pentahydrochloride (MBI 226), a topical 12-amino-acid cationic peptide: spectrum of antimicrobial activity and measurements of bactericidal activity. Antimicrob Agents Chemother. 2004 Aug;48(8):3112-8.

16. Ghiselli R, Giacometti A, Cirioni O, Mocchegiani F, Orlando F, Silvestri C, et al. Efficacy of the bovine antimicrobial peptide indolicidin combined with piperacillin/tazobactam in experimental rat models of polymicrobial peritonitis. Crit Care Med. 2008 Jan;36(1):240-5.

17. Hsu JCY, Yip CM. Molecular dynamics simulations of indolicidin association with model lipid bilayers. Biophys J. 2007 06;92(12):L100-2.

18. Giacometti A, Cirioni O, Barchiesi F, Fortuna M, Scalise G. In-vitro activity of cationic peptides alone and in combination with clinically used antimicrobial agents against Pseudomonas aeruginosa. J Antimicrob Chemother. 1999 Nov;44(5):641-5.

19. Boman HG, Agerberth B, Boman A. Mechanisms of action on Escherichia coli of cecropin P1 and PR-39, two antibacterial peptides from pig intestine. Infect Immun. 1993 Jul;61(7):2978-84.

20. Boman HG. Antibacterial peptides: key components needed in immunity. Cell. 1991 Apr 19;65(2):205-7.

21. Casteels P, Tempst P. Apidaecin-type peptide antibiotics function through a non-poreforming mechanism involving stereospecificity. Biochem Biophys Res Commun. 1994 Feb 28;199(1):339-45.

22. Nagpal S, Kaur KJ, Jain D, Salunke DM. Plasticity in structure and interactions is critical for the action of indolicidin, an antibacterial peptide of innate immune origin. Protein Sci. 2002 Sep;11(9):2158-67.

23. Alfred RL, ShagaghI NM. Tryptophan-rich antimicrobial peptides: properties and applications. Microbial pathogens and strategies for combating them: science, technology and education . 2013:1395-405.

24. Ibrahim MK, Galal AM, Al-Turk IM, Al-Zhrany KD. Antibiotic resistance in Gram-negative pathogenic bacteria in hospitals' drain in Al-Madina Al-Munnawara. Journal of Taibah University for Science. 2010;3(0):14-22.

25. Alexandraki I, Palacio C. Gram-negative versus Gram-positive bacteremia: what is more alarmin(g)? Critical Care. 2010 05/27;14(3):161-.

26. Scott MG, Gold MR, Hancock RE. Interaction of cationic peptides with lipoteichoic acid and gram-positive bacteria. Infect Immun. 1999 Dec;67(12):6445-53.

27. Todar, K. Structure and function of bacterial cells [Internet].; 2012. Accessed Jan 2015. Available from: http://textbookofbacteriology.net/structure_5.html

28. Sigma- Aldrich. Lipopolysaccharides [Internet]; 2014. Accessed Jan 2015. Available from: http://www.sigmaaldrich.com/technical-documents/articles/biology/glycobiology/lipopolysaccharides.html

29. Sigma- Aldrich. Lipopolysaccharides from *Escherichia coli* O111:B4 product information [Internet]; 2013. Accessed Jan 2015. Available from: http://www.sigmaaldrich.com/content/dam/sigma-aldrich/docs/Sigma/Product_Information_Sheet/2/l2630pis.pdf

30. Yu L, Tan M, Ho B, Ding JL, Wohland T. Determination of critical micelle concentrations and aggregation numbers by fluorescence correlation spectroscopy: aggregation of a lipopolysaccharide. Anal Chim Acta. 2006 Jan 18;556(1):216-25.

31. Altria KD. Fundamentals of capillary electrophoresis theory. Methods Mol Biol. 1996 01;52:3-13.

32. UC Davis ChemWiki. Lab 6: Capillary Electrophoresis [Internet]. Accessed Dec 2014. Available from:

http://chemwiki.ucdavis.edu/Wikitexts/UC_Davis/UCD_Chem_115_Lab_Man
ual/Lab_6%3A_Capillary_Electrophoresis

33. Weinberger R. Practical Capillary Electrophoresis. Second ed. San Diego, California: Academic Press; 2000.

34. Vesterberg O. History of electrophoretic methods. J Chromatogr. 1989 Oct 20;480:3-19.

35. Sekhon BS. An overview of capillary electrophoresis : Pharmaceutical , biopharmaceutical and biotechnology applications. J Pharm Educ. 2011;2(2).

36. Tanaka Y, Terabe S. Estimation of binding constants by capillary electrophoresis. J Chromatogr B. 2002 02;768(1):81-92.

37. Schou C, Heegaard NH. Recent applications of affinity interactions in capillary electrophoresis. Electrophoresis. 2006 Jan;27(1):44-59.

38. Vuignier K, Schappler J, Veuthey JL, Carrupt PA, Martel S. Drug-protein binding: a critical review of analytical tools. Anal Bioanal Chem. 2010 Sep;398(1):53-66.

39. Østergaard J, Heegaard NHH. Capillary electrophoresis frontal analysis: principles and applications for the study of drug-plasma protein binding. Electrophoresis. 2003 09;24(17):2903-13.

40. Jiang C, Armstrong DW. Use of CE for the determination of binding constants. Electrophoresis. 2010;31(1):17-27.

41. Scatchard G. Equilibrium in non-electrolyte mixtures. Chem Rev. 1949 Feb;44(1):7-35.

42. Klotz IM. Spectrophotometric investigations of the interactions of proteins with organic anions. J Am Chem Soc. 1946 Nov;68(11):2299-304.

43. Liu X, Dahdouh F, Salgado M, Gomez FA. Recent Advances in Affinity Capillary Electrophoresis (2007). J Pharm Sci. 2008;98(2):394-411.

44. Busch MHA, Carels LB, Boelens HFM, Kraak JC, Poppe H. Comparison of five methods for the study of drug–protein binding in affinity capillary electrophoresis. J Chromatogr A. 1997 8/15;777(2):311-28.

45. Dvorák M, Svobodová J, Benes M, Gas B. Applicability and limitations of affinity capillary electrophoresis and vacancy affinity capillary electrophoresis methods for determination of complexation constants. Electrophoresis. 2013;34(5):761-7.

46. Deeb SE, Wätzig H, El-Hady DA. Capillary electrophoresis to investigate biopharmaceuticals and pharmaceutically-relevant binding properties. TRAC Trend Anal Chem. 2013 0;48(0):112-31.

47. Farmaceutiche S. Capillary coatings in Capillary Electrophoresis (CE) analysis of Biomolecules. . 2008.

48. El-Hady D, Kühne S, El-Maali N, Wätzig H. Precision in affinity capillary electrophoresis for drug–protein binding studies. J Pharm Biomed Anal. 2010 6/5;52(2):232-41.

49. Rundlett KL, Armstrong DW. Examination of the origin, variation, and proper use of expressions for the estimation of association constants by capillary electrophoresis. J Chromatogr A. 1996 1/15;721(1):173-86.

50. Fang N, Chen DDY. Behavior of interacting species in capillary electrophoresis described by mass transfer equation. Anal Chem. 2006;78(6):1832-40.

51. Bowser MT, Sternberg ED, Chen DD. Quantitative description of migration behavior of porphyrins based on the dynamic complexation model in a nonaqueous capillary electrophoresis system. Electrophoresis. 1997 Jan;18(1):82-91.

52. Liu J, Hail M,E., Lee M,S., Abid S, Hangeland J, Zein N. Use of affinity capillary electrophoresis for the study of protein and drug interactions. Analyst. 1998;123(7):1455-9.

53. El-Hady D, Kühne S, El-Maali N, Wätzig H. Precision in affinity capillary electrophoresis for drug–protein binding studies. J Pharm Biomed Anal. 2010 6/5;52(2):232-41.

54. Li Z, Wei C, Zhang Y, Wang D, Liu Y. Investigation of competitive binding of ibuprofen and salicylic acid with serum albumin by affinity capillary electrophoresis. J Chromatogr B. 2011 7/1;879(21):1934-8.

55. Sun Z, Tian L, Lin Q, Ling X, Xiao J, Wang Y. Screening of chemokine receptor CCR4 antagonists by capillary zone electrophoresis. Journal of Pharmaceutical Analysis. 2011 11;1(4):264-9.

56. Li M, Wang Q, Ling X, Yang L, Li Z, Ye M, et al. Interactions Between N-Terminal Extracellular Tail of CCR4 and Natural Products of Licorice Using Capillary Electrophoresis. Chromatographia. 2013 07/01;76(13-14):811-9.

57. Fu H, Li J, Meng W, Dong R, Dai R, Deng Y. Study of binding constant of toll-like receptor 4 and lipopolysaccharide using capillary zone electrophoresis. Electrophoresis. 2011;32(6-7):749-51.

58. Østergaard J, Heegaard NH. Bioanalytical interaction studies executed by preincubation affinity capillary electrophoresis. Electrophoresis. 2006 Jul;27(13):2590-608.

59. Hancock RE, Sahl HG. Antimicrobial and host-defense peptides as new anti-infective therapeutic strategies. Nat Biotechnol. 2006 Dec;24(12):1551-7.

60. Østergaard J, Hansen SH, Jensen H, Thomsen AE. Pre-equilibrium capillary zone electrophoresis or frontal analysis: advantages of plateau peak conditions in affinity capillary electrophoresis. Electrophoresis. 2005 Nov;26(21):4050-4.

61. Jia Z, Ramstad T, Zhong M. Determination of protein-drug binding constants by pressure-assisted capillary electrophoresis (PACE)/frontal analysis (FA). J Pharm Biomed Anal. 2002 10;30(3):405-13.

62. Østergaard J, Heegaard NHH. Capillary electrophoresis frontal analysis: principles and applications for the study of drug-plasma protein binding. Electrophoresis. 2003 09;24(17):2903-13.

CHAPTER 2: PRE-INCUBATION AFFINITY CAPILLARY ELECTROPHORESIS

Introduction

Development of novel drugs is a pressing and world-wide issue due to the emergence of multidrug resistance to presently available antibiotics. A class of drugs known as cationic antimicrobial peptides (CAPs) is showing promise due to their broad spectrum of activity and multiple modes of action resulting in decreased likelihood of them becoming drugs to which resistance is developed (1). Indolicidin (indol) (ILPWKWPWWPWRR-NH_2) is a CAP isolated from the cytoplasmic granules of bovine neutrophils (2). Indol is best known for its short 13-amino acid singular primary structure and high percentage of tryptophan (2, 3). Despite its broad spectrum of antimicrobial, anticancer and antifungal activity, indol has been demarcated for therapeutic use due to its cytotoxic nature (3, 4). The natural structure of indol, however, has represented an excellent starting point for the synthesis of analogues with increased bioactivity and reduced cytotoxicity (4-6). Still, for a derivative of indol to be useful as a therapeutic agent, more information is needed about its precise mechanism of action.

Sequence, charge, size and structure all play a role in indol's activity (7). Many mechanisms of bacterial cell attack have been proposed including (but not limited to) membrane-thinning by disruption of headgroups, inhibition of protein and DNA synthesis, cell leakage via channel formation across the membrane, and stereospecific non-pore forming mechanisms (8-11). For pharmacological purposes, determination of a binding constant (K_b), which provides a ratio of bound to free drug, is an important starting point for drug discovery (12). So far, a K_b for the

interaction of indol with its proposed corresponding receptor, lipopolysaccharide (LPS), has yet to be reported (13).

Use of capillary electrophoresis (CE) for the elucidation of K_b has been steadily increasing and is continuing to gain popularity. Affinity capillary electrophoresis (ACE) is the most widespread CE method currently in use for reporting K_b values with roughly 1000 publication between 2000 to 2012 (14, 15). The ACE study design would require either indol or LPS to be added to the background electrolyte (BGE) in increasing concentrations, while using a constant concentration of the other as a sample with short injection. Preliminary attempts to add indol to the BGE resulted in so much capillary wall adsorption (apparent from the steep baseline) as to render the data useless (Appendix A). Addition of LPS to the BGE yields useable data, however, the molecular mass of LPS is elusive (Sigma Aldrich data sheets claim a mass range of 10-20 kDa), and thus requires the final K_b value to be reported in mg·L^{-1} with assumption of the LPS approximate mass used to make the conversion to L·mol^{-1}. While the conversion could allow for comparison to other literature values, the mass assumption introduces error (See Chapter 3). Pre-incubation ACE (PI-ACE), sometimes termed capillary zone electrophoresis (CZE), involves combining both the protein and the drug for a set amount of time before short injection into the CE. Using this study design, mixing a constant concentration of LPS with increasing concentrations of indol avoids the problem of capillary inner-wall adsorption by introducing lesser quantities of indol to the system and still allows a K_b value to be reported in the standard L·mol^{-1} convention. The K_b is calculated by way of changes in effective electrophoretic mobility (μ_{eff}) which requires a neutral marker of the electroosmotic flow (EOF) in order to compare the

change in electrophoretic mobility of the complex (μ_c) with electrophoretic mobility

of the free protein (μ_f). The following equations are used (16, 17):

$$\mu_{\text{eff}} = \mu_i - \mu_f \qquad \qquad \text{(Eq. 1)}$$

$$\mu_i = \frac{L_d \times L_t}{V}\left(\frac{1}{t_c} - \frac{1}{t_m}\right) \qquad \qquad \text{(Eq. 2)}$$

$$\mu_f = \frac{L_d \times L_t}{V}\left(\frac{1}{t_f} - \frac{1}{t_m}\right) \qquad \qquad \text{(Eq. 3)}$$

μ_{eff} is the effective change in electrophoretic mobility

μ_i is the apparent electrophoretic mobility of the complex

μ_f is the electrophoretic mobility of the free protein (this value is constant for each data set)

L_d is the length of the capillary to the detector window (usually in cm)

L_t is the total length of the capillary (cm)

V is the voltage (V)

t_c is the migration time of the complex (usually in seconds)

t_m is the migration time of the marker (s)

t_f is the migration time of the free protein (s)

Eq. 1 is manipulated to generate plots which serve to determine the value of K_b. The different plotting forms are shown in Table 2.1.

One of the setbacks of using ACE, or in this case PI-ACE, is the assumption of a 1:1 binding stoichiometry. The linear regression plots generated from the PI-ACE data can, however, give indications of different stoichiometries. For instance, it has been suggested that multiple binding is most evident with the linear regression X-reciprocal plot (19). When two distinct trends can be seen, it is indicative of a 2:1

binding interaction (20). A frontal analysis capillary electrophoresis (FACE) study using long injection would be most desirable to eliminate any assumptions of 1:1 binding, however, the study herein represents a modest start to reporting an accurate K_b for the interaction of indol with LPS (For FACE attempts, see Chapter 4).

Table 2.1: Linear regression plotting forms of binding constant (K_b).

Method (synonymous names)	Plotting Equation (y axis vs x axis)	Determination of K_b
X-Reciprocal (Eadie plot, Scatchard plot)	$\dfrac{\mu_{eff}}{[indol]}$ vs μ_{eff}	*-slope*
Y-Reciprocal	$\dfrac{[indol]}{\mu_{eff}}$ vs $[indol]$	$\dfrac{slope}{intercept}$
Double-reciprocal (Lineweaver–Burk plot, Benesi–Hildebrand plot)	$\dfrac{1}{\mu_{eff}}$ vs $\dfrac{1}{[indol]}$	$\dfrac{intercept}{slope}$

μ_{eff} is the change in electrophoretic mobility of the complex, [*indol*] is the indol concentration in μM or M. Table compiled from (16-18).

Experimental

Materials and reagents

Indolicidin at 97.18% purity was purchased from GL Biochem Ltd. in Shanghai, China. LPS isolated from *E.coli* (0111:B4) and monobasic sodium phosphate ($NaH_2PO_4 \cdot H_2O$) were purchased from Sigma-Aldrich, Oakville, Ontario, Canada.

Dibasic sodium phosphate ($Na_2HPO_4 \cdot H_2O$) was obtained from Caledon

Laboratories in Georgetown, Ontario, Canada. DMSO used as EOF marker was from

BDH Chemicals, Toronto, Ontario, Canada. The water used to prepare the solutions

was 18 MΩ water filtered by Barnstead™ Easypure™ RoDi. All reagents used were

of analytical-grade, and all reagents and BGEs were filtered through 0.45-μm

Nylon® syringe filters (Canadian Life Science, ON, Canada). To reduce protein loss

due to adsorption to Nylon® syringe filters, indol and LPS solutions were filtered

with 0.45-μm Cellulose Acetate® syringe filters (Canadian Life Science, ON,

Canada) before introduction to the CE instrument.

BGE and Sample preparation

A pH of 7.2 ± 0.3, resembling physiological pH, was desired for this study. A 100

mM phosphate buffer was prepared by mixing 100 mM dibasic sodium phosphate

($Na_2HPO_4 \cdot H_2O$) and 100 mM monobasic sodium phosphate ($NaH_2PO_4 \cdot H_2O$) to a pH

of 7.3 on the Mettler Toledo FE20 – FiveEasy™ pH meter. This PO_4^{2-} buffer was

stored at room temperature (~23°C).

Stock solutions of 700 mg·L^{-1} LPS and 230 mg·L^{-1} indol were prepared directly in the

100 mM phosphate buffer. The solutions were stored in the refrigerator (~4°C) and

used for a maximum of 30 days. Prior to sample preparation, all stocks and reagents

were filtered using 0.45-μm filters prior to injection into CE. For pre-incubated

samples, in 500 μL sample vials, indol was diluted from 0 to 150 mg·L^{-1} (the

equivalent of 0 to 78.7 (μM) and each was mixed with LPS stock diluted to a

concentration of 50 mg·L^{-1} (of which the equivalent [mol·L^{-1}] is not known). DMSO,

used as a neutral marker, was added to the samples to produce a final concentration

of 0.01% v/v (Table 2.2). Each sample was gently vortexed to ensure even mixing.

To account for incubation time, each sample was made in 15 min increments with

the first sample being analyzed after 2 h and subsequent samples in 15 min intervals thereafter. The samples were then re-analyzed resulting in data collection at 2 ± 0.5 h incubation, 5.5 ± 0.5 h incubation and 10 ± 0.5 h incubation. The concentration ranges used were the result of previous runs indicating the need for this precise range to best represent the interaction.

Table 2.2: Preparation of PI-ACE samples showing volume (µL) of stock LPS, Indol, Buffer and DMSO, and mix time for each sample.

Indol Concentration (mg·L⁻¹)	230 ppm Indol stock (µL)	700 ppm LPS stock (µL) (each sample is 50mg·L⁻¹)	100 mM PO₄²⁻ buffer, pH 7.3 (µL)	0.1% v/v DMSO (µL)	Mix time (±10 min)
0 (DMSO only)	0	0	198	2.0	11:30
0	0	14.3	183.7	2.0	11:45
10	8.7	14.3	175.0	2.0	12:00
20	17.4	14.3	166.3	2.0	12:15
30	26.1	14.3	157.6	2.0	12:30
40	34.8	14.3	148.9	2.0	12:45
50	43.5	14.3	140.2	2.0	13:00
75	65.2	14.3	118.5	2.0	13:15
100	87.0	14.3	96.7	2.0	13:30
150	130.4	14.3	53.3	2.0	13:45

Apparatus

PI-ACE data was collected using a Beckman Coulter ProteomeLab™ PA 800 capillary electrophoresis instrument with ultraviolet (UV) detector set to 214 nm with direct absorbance. A fused-silica capillary from Polymicro Technologies, Phoenix, AZ, USA, of outer diameter 366.0 ± 0.2 µm, inner diameter 50.4 ± 0.2 µm,

48 cm effective length (to detector) and 58 cm total length was used. A circulating liquid fluorocarbon coolant allowed the temperature in the capillary cartridge to be maintained at 25°C.

New capillaries were conditioned with 1.0 M NaOH for 60 min at 20 psi, followed by 0.1 M NaOH for 30 min at 20 psi. Before each new incubation time analysis (every 10 runs), the capillary was flushed with H_2O, 0.1 M NaOH, H_2O, and BGE (each for 10 min at 20 psi of pressure). Prior to each sample injection, the capillary was flushed with 0.1 M NaOH for 4.0 min, H_2O for 2 min, and then BGE for 4 min (each at 20 psi). Rinse steps were extensive to ensure reduction in protein adsorption to the uncoated capillary (18). Normal polarity was used for all runs with voltage set at 20 kV for 10-15 min- enough time to observe all expected outputs. Each sample was injected for 5 s at 1.0 psi. Since the benefit of automation is negated when samples must be prepared in a time-sensitive fashion, samples for this study were only conducted in single runs, with the understanding that any follow-up study would be conducted in triplicate at the incubation time that indicates that equilibrium has been reached.

Results and Discussion

This study was designed to examine the role played by incubation time of samples mixed with both indol and LPS and run under ACE conditions with the ultimate goal of establishing a time at which equilibrium is reached, while generating a preliminary K_b. While most pre-incubation (PI) studies will attempt short incubation times such as 0-90 min (21, 22), preliminary attempts showed changes in complex and free drug mobilities when incubated for 60 min vs. 120 mins.

Appearance of a free indol peak that varied in size indicated a slow equilibrium (23). It became apparent that incubation time would be a major determinant of the final calculated and reported K_b value. This is contrary to some belief that the time-frame of protein-binding equilibration is short (15). The results of 2 h incubation are shown in Figure 2.1. The electropherograms produced for the 5.5 and 10 h incubation times appear very similar to the results for 2 h incubation and it is nearly impossible to visually detect a change in mobility of the LPS·indol complex. The exception is the emergence of the free indol peak around the 40 mg·L^{-1} mark (electropherogram F of Figure 2.1), which tends to vary in size when compared over time (Figure 2.2).

The visual shape and size of the free indol peak does appear to stabilize between the 5.5 and 10 h incubation times, however, calculation of change in electrophoretic mobility (μ_{eff}) shows a slow continued change. μ_{eff} was calculated by collecting the marker and complex peak migration times for each electropherogram to assess the change in mobility in the complex as the LPS binds increasingly more indol. Linear regression plots of double reciprocal, Y-reciprocal, and X-reciprocal were created for each of the three data sets (Table 2.3). Non-linear regression plots were disregarded due to low correlation coefficients ($R^2 \leq 0.6$).
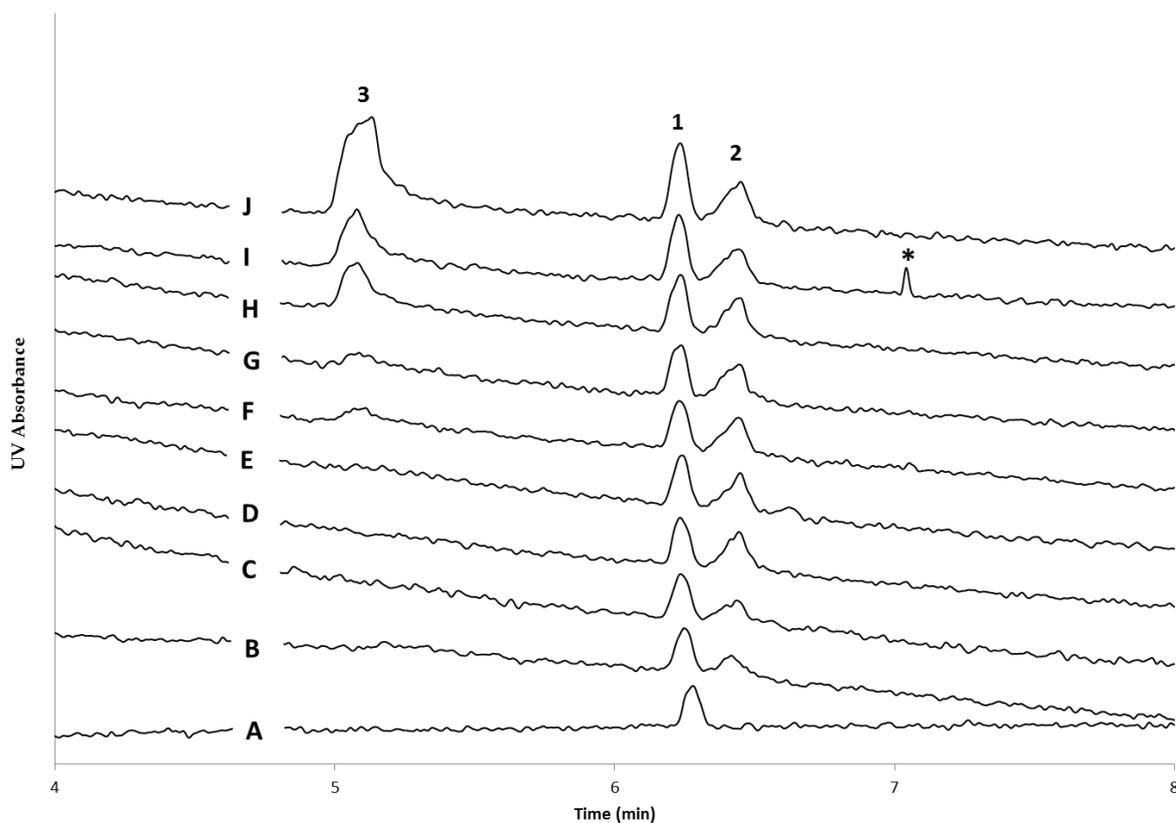
Figure 2.1: Electropherograms of 50 mg·L-1LPS pre-incubated for 2h, mixed with DMSO (0.01 %v/v) and varying concentrations of indol: . A) 0 (DMSO only), B) 0, C) 5.25, D) 10.5, E) 15.7, F) 21.0, G) 26.2, H) 39.3, I) 52.5, and J) 78.7 µM (range is the equivalent of 0-150 mg·L^{-1}). Peak identities: 1) DMSO, 2) LPS/LPS-indol complex, 3) free indol. * is an unknown peak caused by an impurity. CE conditions are described in the Apparatus section.
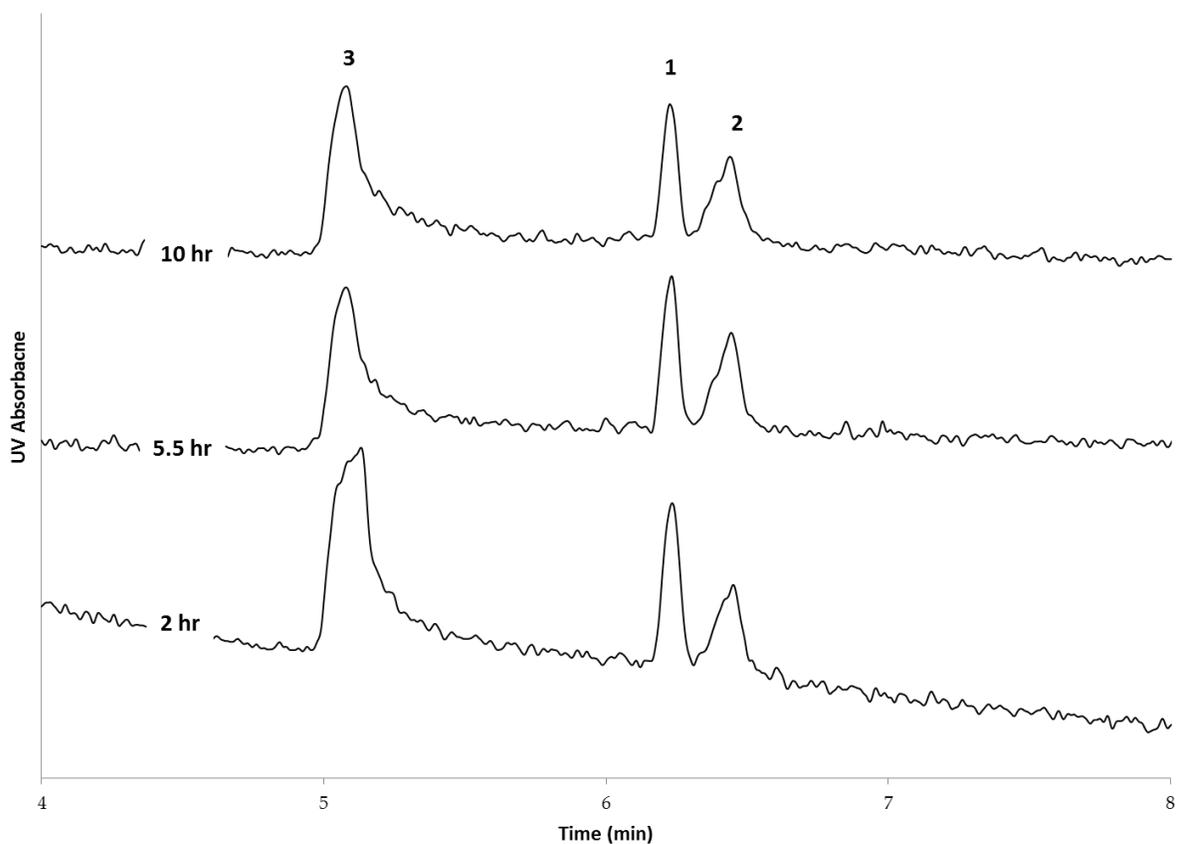
Figure 2.2: Electropherograms at incubation times of 2, 5.5 and 10 hrs, of the same 50 mg·L⁻¹LPS sample pre-incubated with 78.7μM indol (150 mg·L⁻¹) and 0.01 %v/v DMSO as neutral marker. Peak identities: 1) DMSO, 2) LPS/LPS-indol complex, 3) free indol. CE conditions are described in the *Apparatus* section.

Table 2.3: Compilation of regression and binding constant values for 2, 5.5 and 10 h incubation data for the interaction of constant concentration of LPS with varying concentration of indol

Incubation time (hrs ± 0.5)	Regression Type (Reciprocal)	Regression Equation	Correlation (R²)	K_b (M⁻¹) X 10⁵	Average K_b (L·mol⁻¹) X 10⁵
	Double	y = -445.53x - 365.99	0.5536	8.21	
2	Y	y = -344.1x - 988.35	0.9950	3.48	5.22
	X	y = -0.3968x - 0.0012	0.4576	3.97	
	Double	y = -707.89x - 341.28	0.3689	4.82	
5.5	Y	y = -325.24x - 910.82	0.9308	3.57	3.18
	X	y = -0.1137x - 0.0004	0.2330	1.14	
	Double	y = -2762x - 232.3	0.8824	0.84	
10	Y	y = -266.24x - 1548.2	0.9836	1.71	1.11
	X	y = -0.0801x - 0.0004	0.6955	0.80	

The Y-reciprocal plot returned the best R² for each data set with all values above an R² value of 0.9308 (Figure 2.3). The K_b calculated by the regression equation produced by the Y-reciprocal method also most closely resembled the average of the three calculated K_b values. The low R² values of the X-reciprocal plots (Figure 2.4) are the best indication of a stoichiometry that does not fit 1:1 binding, yet the scattering of the data in the X-reciprocal plots does not show 2 or more distinct trends which could allow us to extract multiple binding constants (19, 20). These trends could be more apparent if data for multiple runs is pooled for the optimal

incubation time. The K_b values averaged for all three plotting methods for data collected at 2, 5.5 and 10 h ($\pm$ 0.5) incubations were 5.22 x 10^5 L·mol^{-1}, 3.18 x 10^5, and 1.11 x 10^5 L·mol^{-1} respectively.   Figure 2.6 shows this decreasing average K_b trend graphically. Considering only the three incubation times, the decrease in K_b value appears to occur in a rather linear fashion for the time period of 2-10 h. Additional analyses were conducted with incubation times of ~3-10 h to get a bigger picture of the equilibrium establishment (Figure 2.7). The added data points from these additional incubation times indicate that the equilibrium is reached in the 6-10 h range. The supplemental data gathered also helped to support the K_b findings; indicating that the K_b is in the order of 10^5 L·mol^{-1}. As there has not yet been a K_b reported for the equilibrium interaction between indol and LPS, it is difficult to evaluate the reliability and comparability of these results. The biggest obstacle for reporting a K_b from this data with confidence is the need to perform multiple runs at equilibrium, presumably for samples pre-incubated for six or more hours.
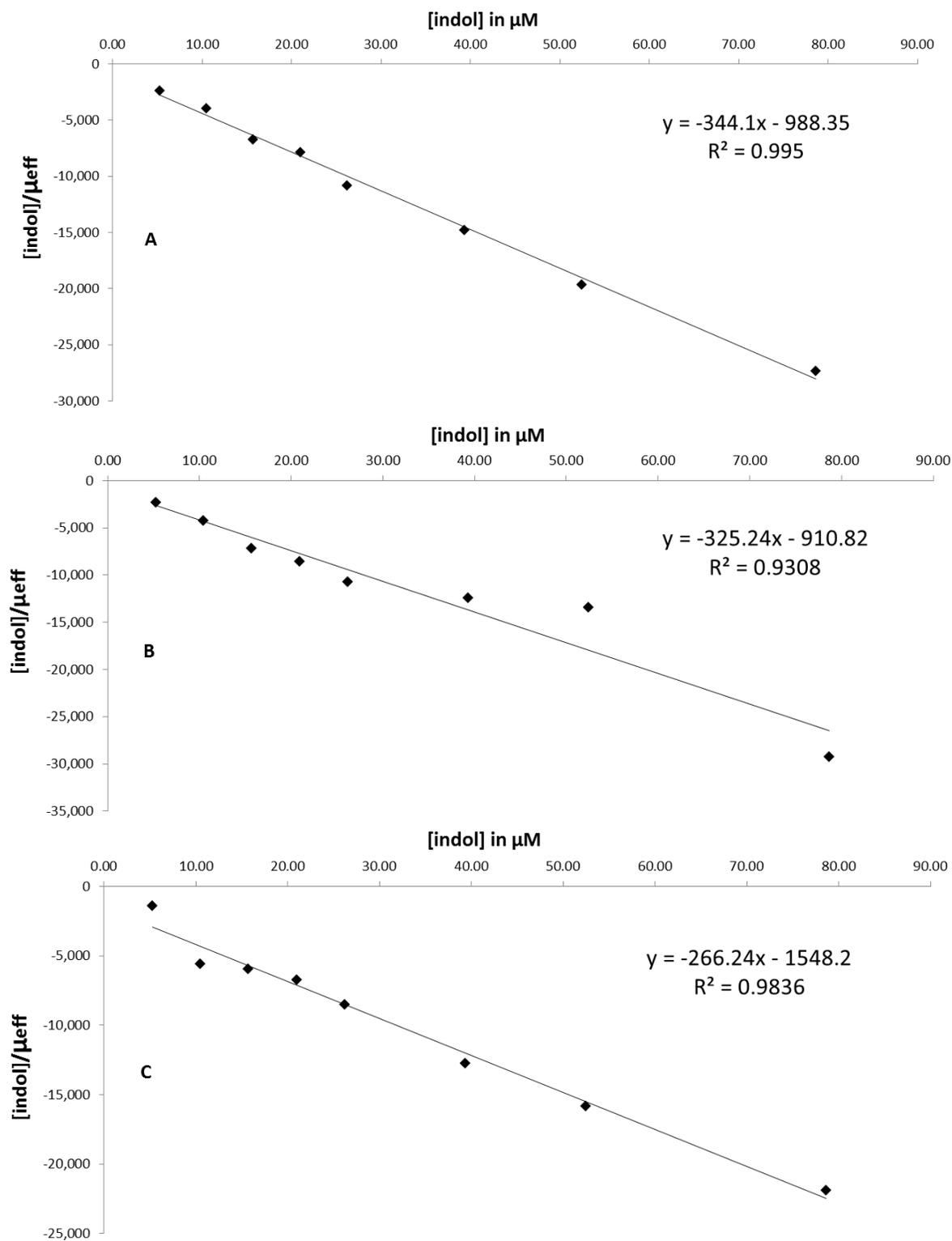
Figure 2.3: The Y-reciprocal plots for A) 2, B) 5.5 and C) 10 h incubation data.
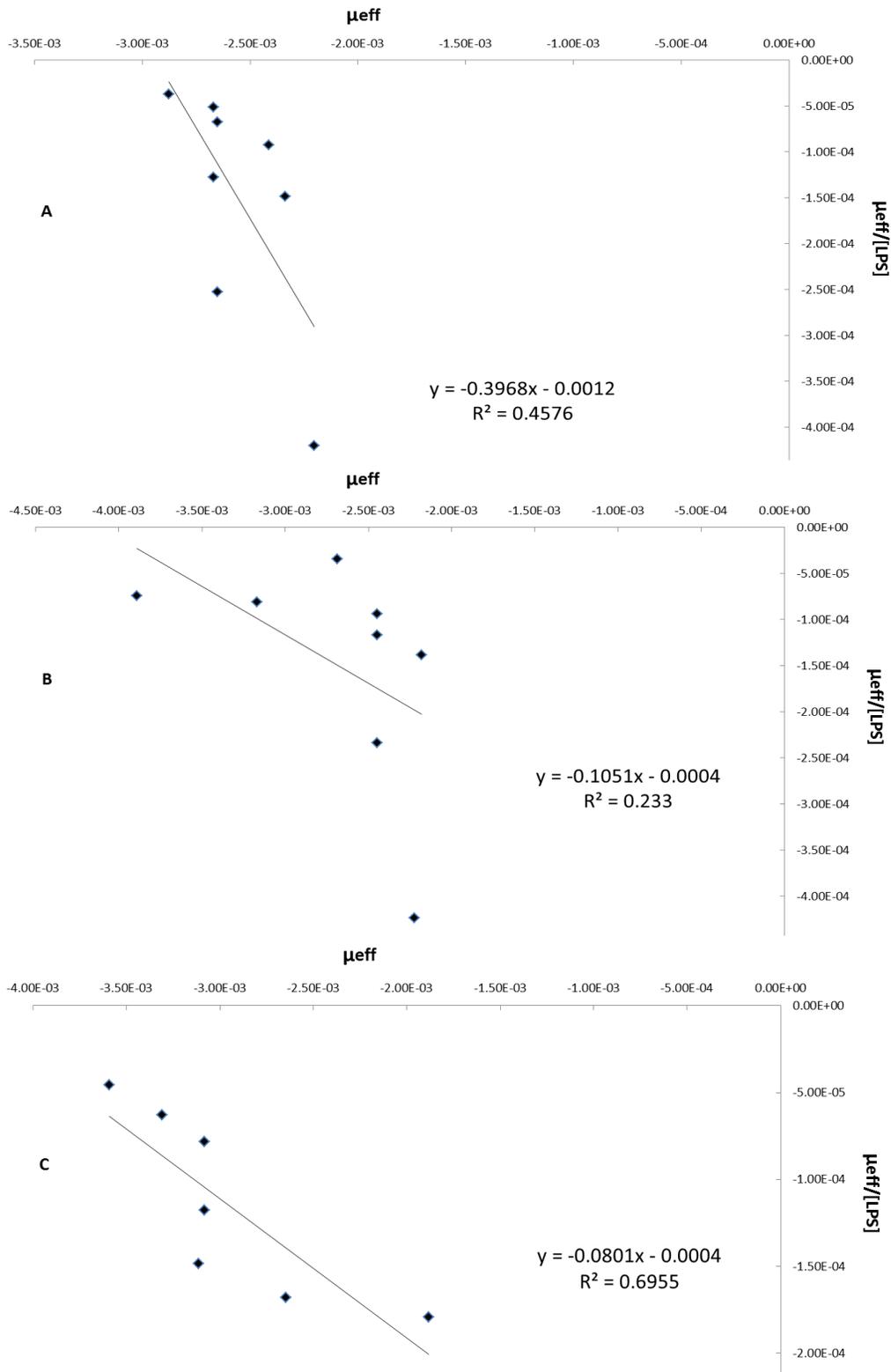
Figure 2.4: The X-reciprocal plots for A) 2, B) 5.5 and C) 10 h incubation data.
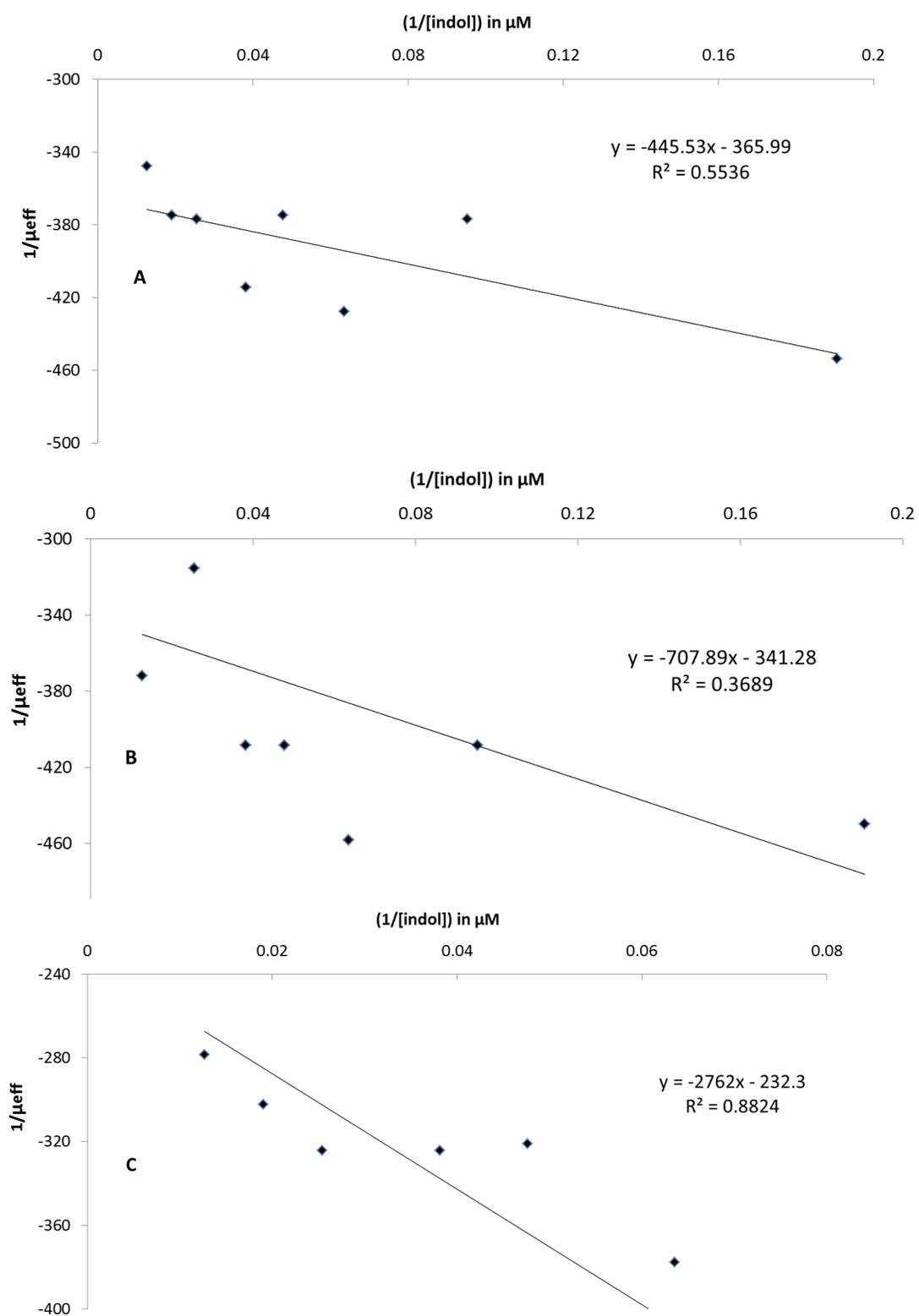
Figure 2.5: The Double-reciprocal plots for A) 2, B) 5.5 and C) 10 h incubation data
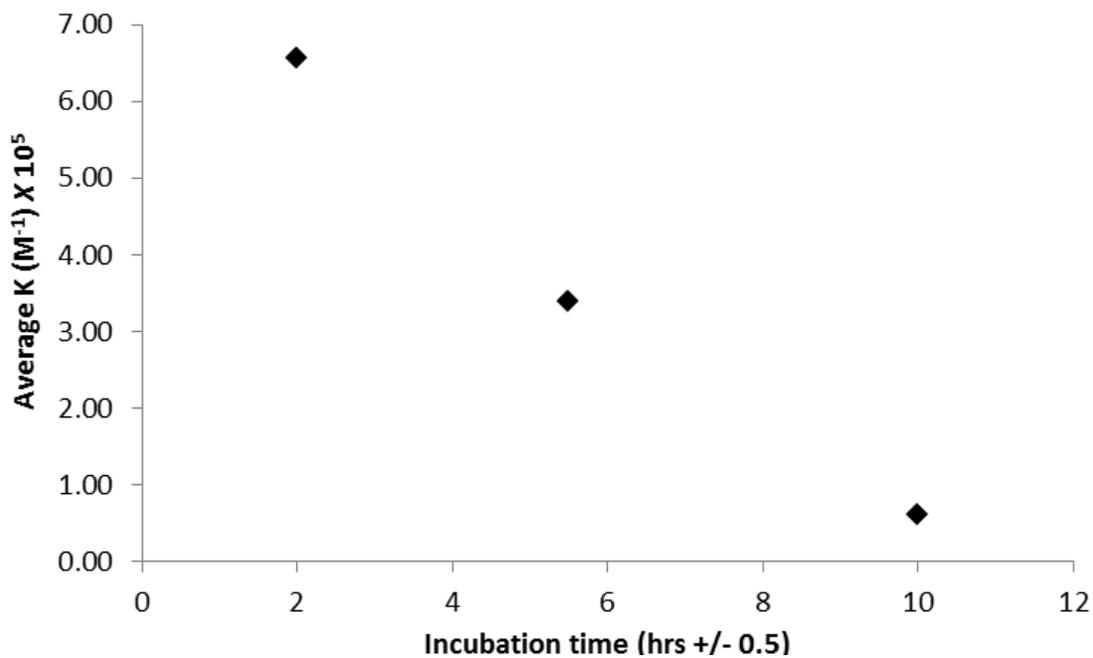
Figure 2.6: Plot of average K_b value trend over time for data collected at 2, 5.5 and 10 h intervals.
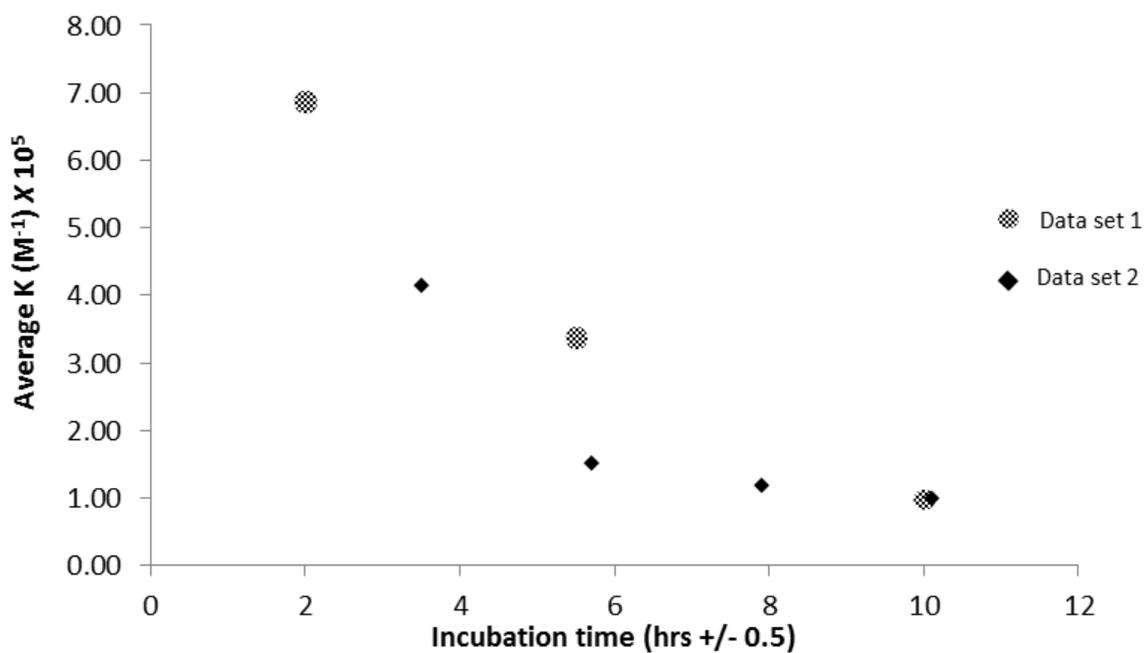
Figure 2.7: Plot of K_b value trend over time compiled for two data sets.

Analyses conducted in Chapter 3 using traditional affinity CE (ACE) shows a K_b in the order of 10^6 L·mol^{-1}, this higher value agrees with the findings in this Chapter due to the short incubation time utilized for the ACE method. Using the PI-ACE method, long incubation times show progressively decreasing K_b values. Using the traditional ACE method requires interaction and equilibration to take place on a much shorter timescale within the capillary. Thus, the combined findings indicate that the largest K_b value is achieved for lesser amounts of incubation time. Since in both ACE and PI-ACE, the fraction of bound drug is estimated based on the mobility of the bound versus unbound species, the larger K_b value indicates a more "sluggish" complex that is being slowed down by more interactions with the drug (indol). A hypothesized visual depiction of the interaction between indol and LPS is shown in Figure 2.8. It is assumed that the receptor, LPS forms a micelle in an aqueous environment which mimics a cell membrane. When indol first interacts with the LPS micelle, it is at the periphery of the micelle presumably using electrostatic interactions between the cationic amino acids of indol and the anionic phosphate groups of LPS. The mobility of the complex is at this time more greatly affected by the location of the indol binding. Once the electrostatic interaction binds indol and LPS, the hydrophobic regions of indol (namely tryptophan) interact with the LPS micelle to penetrate the membrane. As this interaction occurs, the indol are further from the periphery of the LPS micelle and thus are not as greatly affecting the complex's mobility. Finally, once indol has penetrated the micelle membrane, it is compromised and indol is able to bypass into the micelle, thus resulting in a less affected mobility of the complex. This hypothesis would explain the progressive decrease in K_b value as incubation time is increased.

Schematic representation of **indolicidin**. Blue indole unit represents hydrophobic amino acids, green portion represents cationic amino acids.

Schematic representation of **LPS**. Red portion is hydrophobic lipid head group. Black "tail" is hydrophilic sugars.

Schematic representation of a **micelle** formed from LPS units.

The positively charged portions of indol bind to the negatively charged phosphate groups at the hydrophilic interface by electrostatic interaction.

Highest K_b, mobility most greatly affected

The hydrophobic portion of indol, namely the tryptophan residues, imbed themselves into the micelle membrane by hydrophobic interaction.
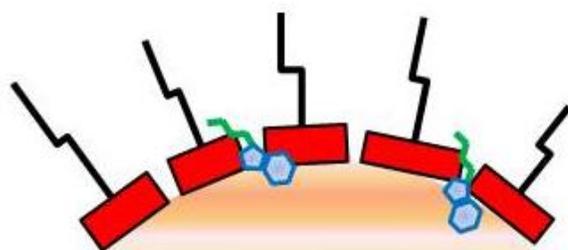
Moderate K_b, mobility moderately affected

The disruption to the micellar membrane by hydrophobic interactions allows indol to penetrate and enter the micelle.
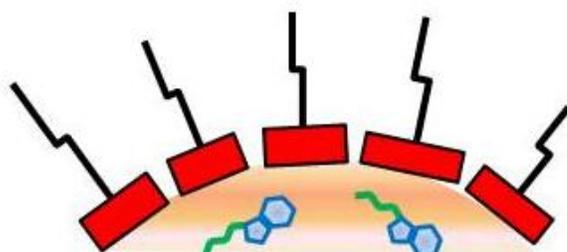
Lowest K_b, mobility least affected

Figure 2.8: Hypothetical sequence of events for interaction of indol with an LPS micelle.

Conclusion

For this study, samples containing increasing concentrations of indol and a constant concentration of LPS were pre-incubated for 2, 5.5 and 10 h ($\pm$0.5) and analyzed under the same CE conditions to provide preliminary K_b values and shed light on the effect of incubation time. The results showed a clear indication of binding, evident by the appearance of a free indol peak once the LPS was saturated. The binding was also supported by the change in electrophoretic mobility of the LPS/LPS-indol complex as increasing concentrations of indol were added. For a preliminary data-set, a total of nine K_b values were produced: one for each of double, X-, and Y-reciprocal plots for each of the three incubation times assessed. The average of the three K_b values produced from the three regression plots was 5.22 x 10^5, 3.18 x 10^5, and 1.11 x 10^5 L·mol^{-1} for 2, 5.5 and 10 h ($\pm$ 0.5) incubations, respectively. The best correlations were generated by the Y-reciprocal plots, with R^2 values of $\geq$ 0.9308. The double reciprocal and X-reciprocal plots had lower R^2 values, the lowest value being of 0.2330 for the X-reciprocal plot of 5.5 hour incubation data. This low R^2 could be indicative of multiple binding stoichiometries (19). Collection of additional data supported the K_b values and showed that equilibrium is reached beyond six hours; therefore, a more definitive conclusion of the binding stoichiometries could be drawn if more replicates of the study were conducted at this same incubation time. A trend of decreasing K_b is corroborated by the findings of Chapter 3 which give a higher preliminary K_b finding in the order of 10^6 L·mol^{-1} when samples are not pre-incubated at all. Furthermore, the use of FACE, if conducted successfully, would give a much more reliable K_b value because FACE analysis is not limited to 1:1 binding (24).

Continued work in this field would greatly benefit from determining an approximate molecular weight for LPS, which could be applied to the use of either traditional ACE or FACE where the LPS concentration could be varied. The resulting K_b value could then be reported in $L \cdot mol^{-1}$ without assumptions needing to be made for LPS mass. Reproduction of this study with multiple replicates could generate more data and perhaps a more confident K_b determination, however, the setup of this study is very tedious with samples needing to be made repeatedly and on a strict time-frame, making accurate reproduction of incubation time data difficult. Determining that equilibrium is in fact established would alleviate the strictness currently required for this parameter, allowing for ease of automation and more flexibility with time at which samples are mixed. ACE and FACE would also benefit the researcher with the use of instrument automation, and greatly simplify the study design. A traditional ACE pilot study is discussed in Chapter 3, while attempts to perform FACE on the indol-LPS system is discussed in Chapter 4.

References

1. Hancock RE, Sahl HG. Antimicrobial and host-defense peptides as new anti-infective therapeutic strategies. Nat Biotechnol. 2006 Dec;24(12):1551-7.

2. Selsted ME, Novotnytll MJ, Morris WL, Tang Y, Smith W, Cullor JS. Indolicidin, a novel bactericidal tridecapeptide amide from neutrophils. J Biol Chem. 1991;267(7):4292-5.

3. Alfred RL, ShagaghI NM. Tryptophan-rich antimicrobial peptides: Properties and applications. Microbial pathogens and strategies for combating them: science, technology and education. 2013:1395-405.

4. Podorieszach AP, Huttunen-Hennelly H. The effects of tryptophan and hydrophobicity on the structure and bioactivity of novel indolicidin derivatives with promising pharmaceutical potential. Org Biomol Chem. 2010 04;8(7):1679-87.

5. Bhargava A, Osusky M, Hancock RE, Forward BS, Kay WW, Misra S. Antiviral indolicidin variant peptides: Evaluation for broad-spectrum disease resistance in transgenic nicotiana tabacum. Plant Science. 2007 3;172(3):515-23.

6. Sader HS, Fedler KA, Rennie RP, Stevens S, Jones RN. Omiganan pentahydrochloride (MBI 226), a topical 12-amino-acid cationic peptide: Spectrum of antimicrobial activity and measurements of bactericidal activity. Antimicrob Agents Chemother. 2004 Aug;48(8):3112-8.

7. Krajewski K, Marchand C, Long YQ, Pommier Y, Roller PP. Synthesis and HIV-1 integrase inhibitory activity of dimeric and tetrameric analogs of indolicidin. Bioorg Med Chem Lett. 2004 Nov 15;14(22):5595-8.

8. Hsu JCY, Yip CM. Molecular dynamics simulations of indolicidin association with model lipid bilayers. Biophys J. 2007 06;92(12):L100-2.

9. Boman HG, Agerberth B, Boman A. Mechanisms of action on *Escherichia coli* of cecropin P1 and PR-39, two antibacterial peptides from pig intestine. Infect Immun. 1993 Jul;61(7):2978-84.

10. Boman HG. Antibacterial peptides: Key components needed in immunity. Cell. 1991 Apr 19;65(2):205-7.

11. Casteels P, Tempst P. Apidaecin-type peptide antibiotics function through a non-poreforming mechanism involving stereospecificity. Biochem Biophys Res Commun. 1994 Feb 28;199(1):339-45.

12. Vuignier K, Schappler J, Veuthey JL, Carrupt PA, Martel S. Drug-protein binding: A critical review of analytical tools. Anal Bioanal Chem. 2010 Sep;398(1):53-66.

13. Nagpal S, Kaur KJ, Jain D, Salunke DM. Plasticity in structure and interactions is critical for the action of indolicidin, an antibacterial peptide of innate immune origin. Protein Sci. 2002 Sep;11(9):2158-67.

14. Dvorák M, Svobodová J, Benes M, Gas B. Applicability and limitations of affinity capillary electrophoresis and vacancy affinity capillary electrophoresis methods for determination of complexation constants. Electrophoresis. 2013;34(5):761-7.

15. Deeb SE, Wätzig H, El-Hady DA. Capillary electrophoresis to investigate biopharmaceuticals and pharmaceutically-relevant binding properties. TRAC Trend Anal Chem. 2013 0;48(0):112-31.

16. Rundlett KL, Armstrong DW. Examination of the origin, variation, and proper use of expressions for the estimation of association constants by capillary electrophoresis. J Chromatogr A. 1996 1/15;721(1):173-86.

17. Tanaka Y, Terabe S. Estimation of binding constants by capillary electrophoresis. J Chromatogr B, Analytical technologies in the biomedical and life sciences. 2002 02;768(1):81-92.

18. El-Hady D, Kühne S, El-Maali N, Wätzig H. Precision in affinity capillary electrophoresis for drug–protein binding studies. J Pharm Biomed Anal. 2010 6/5;52(2):232-41.

19. Bowser MT, Sternberg ED, Chen DD. Quantitative description of migration behavior of porphyrins based on the dynamic complexation model in a nonaqueous capillary electrophoresis system. Electrophoresis. 1997 Jan;18(1):82-91.

20. Liu J, Hail M,E., Lee M,S., Abid S, Hangeland J, Zein N. Use of affinity capillary electrophoresis for the study of protein and drug interactions. Analyst. 1998;123(7):1455-9.

21. Zhang YW, Yan HY, Fu P, Jiang F, Zhang Y, Wu WX, et al. Modified capillary electrophoresis based measurement of the binding between DNA aptamers

and an unknown concentration target. Anal Bioanal Chem. 2013 Jun;405(16):5549-55.

22. Farmaceutiche S. Capillary coatings in capillary electrophoresis (CE) analysis of biomolecules. 2008.

23. Østergaard J, Heegaard NHH. Capillary electrophoresis frontal analysis: Principles and applications for the study of drug-plasma protein binding. Electrophoresis. 2003 09;24(17):2903-13.

24. Vuignier K, Schappler J, Veuthey J, Carrupt P, Martel S. Improvement of a capillary electrophoresis/frontal analysis (CE/FA) method for determining binding constants: Discussion on relevant parameters. J Pharm Biomed Anal. 2010 12;53(5):1288-97.

CHAPTER 3: TRADITIONAL AFFINITY CAPILLARY ELECTROPHORESIS

Introduction

Indolicidin (indol) (ILPWKWPWWPWRR-NH$_2$) is a cationic antimicrobial peptide (CAP) isolated from the cytoplasmic granules of bovine neutrophils (1). CAPs, also termed simply antimicrobial peptides (AMPs), are showing some promise in the search for new drug candidates due to their incredible spectrum of activity coupled with their ability to employ multiple modes of action against pathogens (2). Antibiotic resistance is thought to be less likely to occur when a drug uses multiple actions to achieve an antimicrobial result. Cytotoxicity has prevented advancement of indol in drug development; however, solutions have been presented. Using the natural structure of indol, derivatives can be created with equivalent or increased antimicrobial properties and reduced cytotoxicity (3-5). Drug development is benefitted by the elucidation of a binding constant (K$_b$) which can indicate the fraction of free versus bound drug. A value of K$_b$ has not yet been published for the interaction of indol with its proposed receptor, lipopolysaccharide (LPS) (6). Comparison of elucidated K$_b$s to other methods of K$_b$ determination (ie. spectroscopic approaches, isothermal titration calorimetry (ITC)) is recommended (7). These comparisons are often done within the same research group or laboratory; however, this is not possible for the current research. Nevertheless, a large K$_b$ for this interaction would add credence to the assumption that entry into a bacterial cell is via LPS as receptor and would be a step towards reporting the type of non-covalent interaction which could be elucidated by a thermodynamic study.

Affinity capillary electrophoresis (ACE) is one of the best known and most commonly used methods of K_b determination (8). Capillary electrophoresis (CE) is an excellent analytical tool due to its high separation efficiency, high resolving power, quick analysis time, low injection volume, and ability to automate (9). The ACE study design is popular because it is very simple. For our purposes, either indol or LPS can be added to the background electrolyte (BGE) while the other is injected into the capillary as a sample. During initial research, it was found that addition of indol to the BGE was not a feasible study design owing to the cationic nature of indol which resulted in heavy adsorption to the bare fused silica inner capillary walls (see Appendix A). A cationic capillary coating of hexadimethrine bromide and dextran (PB-DS-PB coating) was attempted to limit protein interaction with capillary walls, however the results were poor. A bare fused silica capillary was used with special attention to rinse protocols as outlined by El-hady *et al* [2010] (10). Thus, the LPS was added in increasing concentrations to the run buffer and indol was injected as a sample. All other CE parameters are kept constant while equilibration takes place within the capillary. A variety of K_b values are revealed by producing linear regression plots from calculation of effective electrophoretic mobility (μ_{eff}), which is the change in electrophoretic mobility of free (μ_f) compared to complexed species (μ_c) (11). The linear regression plots are the double reciprocal, Y-reciprocal and X-reciprocal plots. In ACE, these plots assume a linear trend and 1:1 binding stoichiometry (12). A binding stoichiometry that differs from 1:1 is best indicated on an X-reciprocal plot, also known as a Scatchard analysis, by non-linearity or presence of two distinct trends (11, 13).

Studies such as this one aim to achieve a better understanding of the mechanism of action of a drug by evaluating the strength of its binding to its corresponding

receptor. It is acknowledged that simplifying an interaction study to only include a drug and one receptor ignores the effect of many biological features such as membrane potential, pH gradients, lipid heterogeneity, the presence of membrane proteins and more (14). Still, it is accepted that such studies are helpful for gleaning a broad overview of interaction mechanisms. Conducting the ACE interaction study of indol with LPS at the physiological pH of ~7.4 was challenging due to the cationic nature of indol, but helps to substantiate the significance of the results. A preliminary K_b range is reported from the results of this ACE study, representing progression to a better understanding of the interaction between the CAP indol and its proposed ligand, LPS.

Experimental

Materials and reagents

Indolicidin (97.18% pure) was purchased from GL Biochem Ltd. in Shanghai, China. LPS isolated from *E.coli* (0111:B4) and monobasic sodium phosphate ($NaH_2PO_4 \cdot H_2O$) were purchased from Sigma-Aldrich, Oakville, Ontario, Canada. Dibasic sodium phosphate ($Na_2HPO_4 \cdot H_2O$) was obtained from Caledon Laboratories in Georgetown, Ontario, Canada. DMSO used as EOF marker was obtained from BDH Chemicals, Toronto, Ontario, Canada. The water used to prepare the solutions was 18 MΩ water filtered by Barnstead™ Easypure™ RoDi. All reagents used were of analytical-grade, and all reagents and background electrolytes (BGEs) were filtered through 0.45-µm Nylon® syringe filters (Canadian Life Science, ON, Canada). To reduce protein loss due to adsorption to Nylon® syringe filters, indol and LPS solutions were filtered with 0.45-µm Cellulose

Acetate® syringe filters (Canadian Life Science, ON, Canada) before introduction to the CE instrument.

BGE and Sample preparation

To be applicable to physiological systems, a pH of 7.2 (+/- 0.3) was desired for this study. The stock phosphate buffer was prepared by mixing 100 mM dibasic sodium phosphate ($Na_2HPO_4 \cdot H_2O$) and 100 mM monobasic sodium phosphate ($NaH_2PO_4 \cdot H_2O$) to a pH of 7.3 on the Mettler Toledo FE20 – FiveEasy™ pH meter. The resulting buffer was stored at room temperature ($\sim 23^oC$) and used for no more than 30 days.

Stock solutions of LPS and indol were prepared by dissolving analytically weighed fluffy white solid directly into the 100 mM phosphate buffer to final concentrations of 420 mg·L^{-1} and 230 mg·L^{-1}, respectively. The solutions were stored in the refrigerator ($\sim 4^oC$) and used for a maximum of 30 days. Prior to sample preparation, all stocks and reagents were filtered using 0.45-μm filters prior to injection into CE. A single indol sample, of concentration 50 mg·L^{-1} was made from indol stock by dilution with phosphate buffer. DMSO, used as a neutral marker, was added to this sample to produce a final concentration of 0.01% v/v in a 500 μL sample vial. BGE for this study consisted of concentrations of LPS from 0 to 150 mg·L^{-1} dissolved in 100 mM phosphate buffer (Table 3.1). The indol sample as well as the inlet and outlet vials of LPS consisting buffer were gently vortexed to ensure even mixing.

Table 3.1: Preparation of LPS containing BGE showing volumes of LPS and buffer.

LPS concentration in BGE (mg·L⁻¹)	420 mg·L⁻¹ LPS stock (µL)	100 mM PO₄²⁻ buffer, pH 7.3 (µL)
0	0	1000
25	59.5	940.5
75	178.5	821.5
150	357.0	643.0

Apparatus

Traditional ACE data was collected using a Beckman Coulter ProteomeLab™ PA 800 capillary electrophoresis instrument with detection at 214 nm with an ultraviolet (UV) detector set at direct absorbance. A fused-silica capillary from Polymicro Technologies, Phoenix, AZ, USA, of outer diameter 366.0 ± 0.2 µm, inner diameter 50.4 ± 0.2 µm, 48cm effective length (to detector) and 58 cm total length was used. A circulating liquid fluorocarbon coolant allowed the temperature in the capillary cartridge to be maintained at 25°C.

New capillaries were conditioned (each at 20 psi) with 1.0 M NaOH for 60 min, followed by 0.1 M NaOH for 30 min. Before the sequence was started, the capillary was flushed (each for 10 mins at 20 psi of pressure) with H_2O, 0.1 M NaOH, H_2O, and plain 100 mM phosphate buffer (pH 7.3). Prior to each sample injection, the capillary was flushed (each at 20 psi) with 0.1 M NaOH for 4 min, H_2O for 2 min, and then phosphate buffer for 4 min. Extensive use of rinse steps was used to ensure reduction in protein adsorption to the uncoated capillary (15). Normal polarity was used for all runs with voltage set at 10 kV for 20-30 min, enough time to

observe all expected peaks in the output electropherograms. Each sample was injected for 5 s at 1.0 psi. All samples were analyzed in duplicate.

Results and Discussion

This study was designed as a pilot project to see the outcomes when traditional ACE is conducted using indol as the sample and LPS dissolved in the BGE. Calculation of a preliminary K_b while using LPS as the varying component limits the precise reported K_b value to mg·L^{-1}, due to the ambiguity behind the molar mass of LPS (Sigma Aldrich reports a mass range of 10-20 kDa)(16). This approach is still preferred because conducting the study in reverse, by placing indol in the BGE, results in excessive adsorption to the inner walls of the capillary by introducing high concentrations of cationic indol into the system (See Appendix A). It is also advantageous to keep the indol concentration constant and low to further reduce protein wall adsorption. In addition, it is feasible to convert the reported K_b from L·mg^{-1} to L·mol^{-1} by using the estimated mass range of 10 kg to 20 kg·mol^{-1} that is suggested by Sigma Aldrich. Using this approach certainly introduces error and a number of questions surrounding the accuracy of the LPS mass estimation, however, a large K_b value can still lend support to the assumption that LPS is the probable receptor for indol when entering a cell. The compiled electropherograms shown in Figure 3.1 were produced in duplicate and both sets of data look nearly identical.
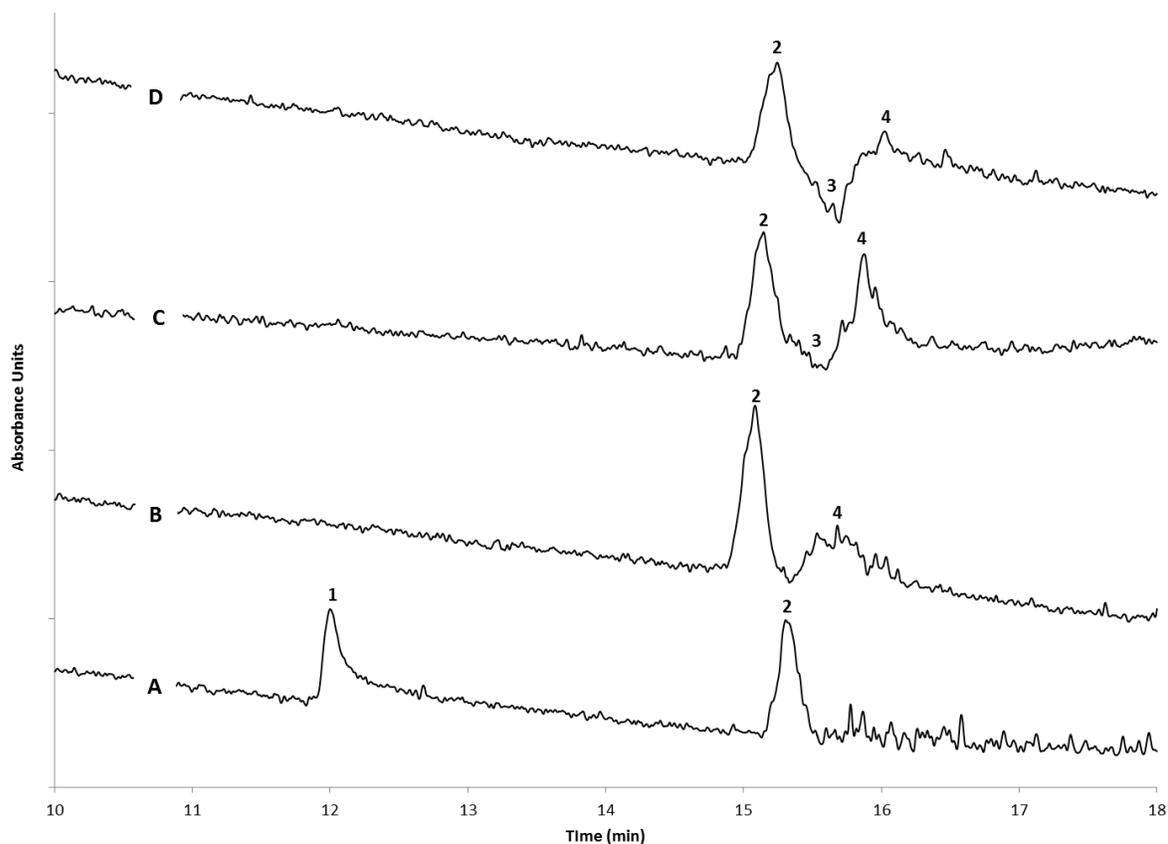
Figure 3.1: Electropherograms of 50 mg·L^{-1} (26.2 µM) indol and DMSO (0.02%v/v) analyzed with varying concentrations of LPS added to the 100 mM phosphate BGE. LPS concentrations in buffer are A) 0, B) 25, C) 75, and D) 150 mg·L^{-1}. Peak identities: 1) free indol, 2) DMSO, 3) LPS vacancy trough, 4) is the LPS/LPS-indol complex. CE conditions are described in the *Apparatus* section.

The disappearance of the indol peak immediately upon addition of just 25 mg·L^{-1} LPS to the run buffer is an excellent indication of an interaction between indol and LPS. As more LPS is delivered to the capillary via higher concentration in the buffer, the complex peak grows marginally and a vacancy peak (or trough) presents itself. This trough indicates that LPS is being removed from the BGE and becoming part of a complex resulting in a lower absorbance in the region of LPS's migration time. The visual trend is deceiving as the complex size seems larger for the BGE with 75

mg·L^{-1} LPS as compared to the complex when 150 mg·L^{-1} is present in the BGE (Figure 3.1 **C** vs. **D**). The calculations of change in mobility of the indol·LPS complex verify that in fact the mobility of the complex is proportionally changed with increasing concentrations of LPS in the run buffer. Changes in viscosity of the BGE, which can themselves influence changes in migration time are easily accounted for by multiplying effective electrophoretic mobility μ_{eff} by the ratio (I_o/I), where I_o is the current without any additives in the buffer solution and I is the current when there is additive in the buffer solution (17). For these analyses, the changes in current with LPS in the BGE were so minor as to be deemed insignificant ($I_o/I \geq 0.987$).

The data gathered from the two replicates of this study were pooled and used to create double reciprocal, Y-reciprocal and X-reciprocal linear regression plots (Figure 3.2). The resulting K_b values are shown in Table 3.2. As is often the case, the Y-reciprocal data shows the highest correlation coefficient ($R^2 = 0.9999$), while the X-reciprocal method has a much lower R^2 value ($R^2 = 0.7807$) (7). This is an indication that the binding stoichiometry should not be assumed to be 1:1 (13). In a follow-up to this pilot study, use of the recommended seven different receptor concentrations should be utilized, which could allow use of the X-reciprocal analysis to infer two K_b values, rather than just one (10, 11).
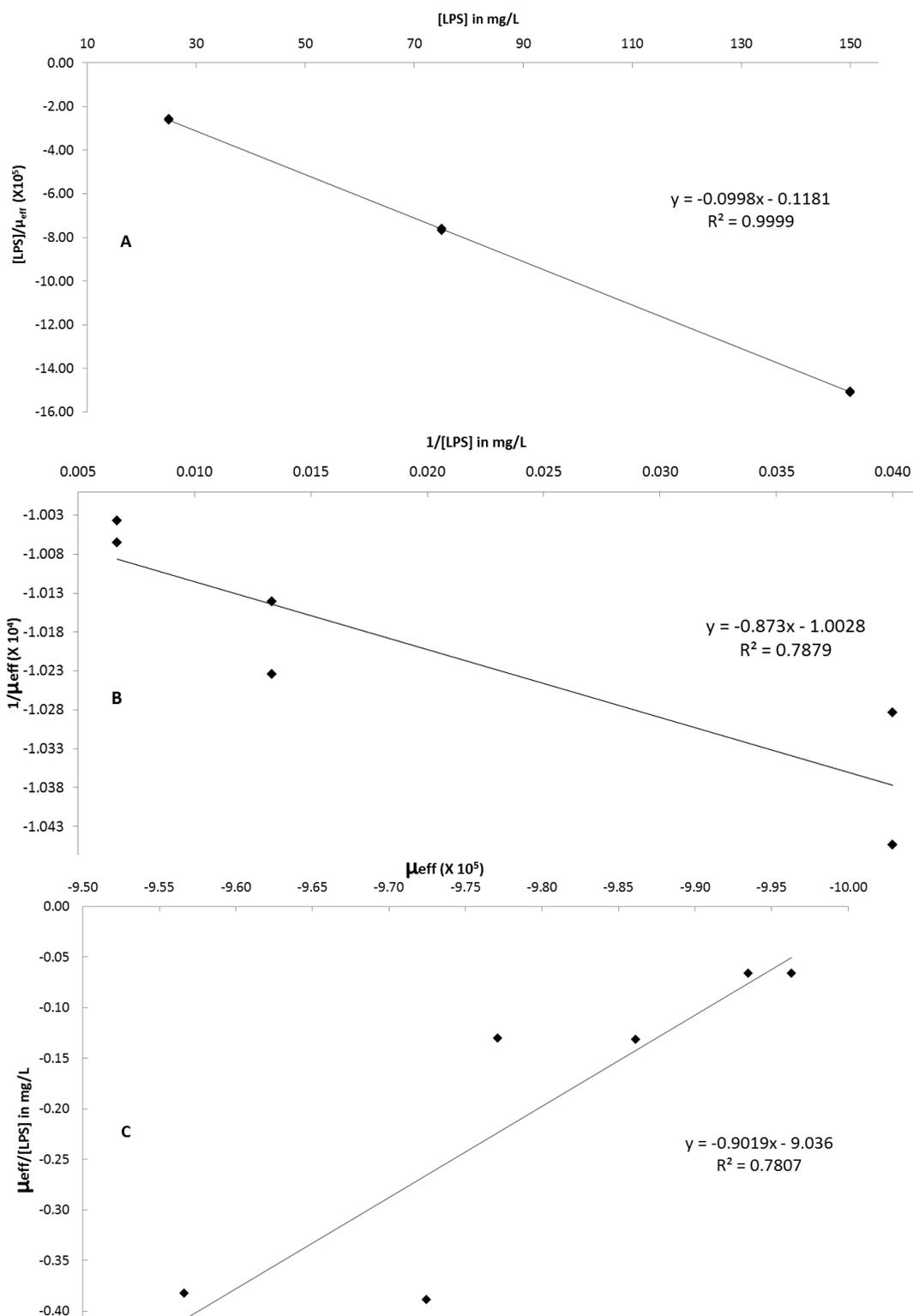
Figure 3.2: (A) Y-reciprocal, (B) Double reciprocal and, (C) X-reciprocal plots of the ACE interaction between indol and LPS. n=6 for each plot. In plot A, 3 additional points are unseen because they are exactly overlapping.

Use of the LPS mass range reported by Sigma-Aldrich allows the conversion of the K_b value from the less useful $mg \cdot L^{-1}$ to $mol \cdot L^{-1}$. The 10-20 kDa value is suggested for intact bacterial LPS [16]. From Table 3.2, it can be seen that converting the average from 0.962 $mg \cdot L^{-1}$ gives us the K_b range of 9.62- 19.2 x 10^6 $L \cdot mol^{-1}$. The large K_b suggests that in the LPS-indol interaction equilibrium the reaction lies in the direction of the products (*i.e.*, the complex is heavily favoured). Further investigations of LPS molecular mass have reported 50-100 kDa when it is treated with sodium dodecyl sulfide (SDS) and heat [18]. The mass is even greater when considering the formation of micelles, which can result in aggregate masses upwards of 1000-4000 kDa. The critical micelle concentration for LPS isolated from *E.coli* (0111:B4) is reported as 1.3-1.6 μM (the equivalent of 13-16 $mg \cdot L^{-1}$-assuming 10 kDa) and is likely to form aggregates of 43-49 molecules per micelle [19]. Selection of a suitable LPS mass for the unit conversion will affect the K_b outcome by several orders of magnitude. From an estimated LPS mass range of 10-4000 kDa, we arrive at a K_b range of 9.62 x 10^6 to 3.85 x 10^9 $L \cdot mol^{-1}$. While this is an enormous range, even the lowest value is indicative of an equilibrium favouring the products. At the concentrations used in this study, LPS micelle formation is inevitable, and thus it is almost certain that we are dealing with a high and variable molecular mass [20]. The variability is a combination of the heterogenous nature of LPS structures, and also the variations in aggregate formation [16]. Despite the uncertainty associated with LPS molecular mass, we can be certain that the mass is at minimum 10-20 kDa, and given the published literature suggesting aggregates of 43-49 LPS units per micelle, the upper mass estimate is likely closer to 980 kDa. The result is a final K_b value that is at very minimum 9.62 x 10^6 $L \cdot mol^{-1}$, definitely in favour of the complex.

Table 3.2: Compilation of regression and binding constant values for linear regression plots of traditional ACE data for the interaction of indol with LPS

Regression Type (Reciprocal)	Regression Equation	Correlation (R^2)	K_b ($mg·L^{-1}$)	Avg K_b ($mg·L^{-1}$)	Adjusted with 10kDa LPS mass ($L·mol^{-1}$)	Adjusted with 20kDa LPS mass ($L·mol^{-1}$)
Double	y = -0.873x - 1.0028	0.7879	1.14			
Y	y = -0.0998x – 0.1811	0.9999	0.845	0.962	9.62×10^6	19.2×10^6
X	y = -0.9019x - 9.036	0.7807	0.902			

Initially, the baseline resolution of these findings, namely the lack of spacing between DMSO, the LPS trough and the indol/LPS complex seen in Figure 3.1, seemed unacceptable for use with K_b calculations; however, comparison to published electropherograms indicated otherwise (21). Given the success of these pilot runs, it would definitely be advisable for the study to be reproduced with collection of a larger data set. For a more confident result, upwards of seven concentrations of LPS in the BGE in total is advised, and conducted in triplicate with standard deviation reported (7, 10) . Had the usefulness of these findings been recognized sooner, additional data would already have been collected, alas efforts at the traditional ACE study method were abandoned before this data was fully understood and analyzed.

Conclusion

A traditional ACE pilot study was implemented for investigation of the interaction between the AMP indol and its proposed receptor, LPS. The indol sample

concentration remained constant while the concentration of LPS dissolved in BGE was varied. All other CE parameters remained constant. The results showed a clear indication of binding, evident by the disappearance of the free indol peak once LPS was present in the BGE. A change in electrophoretic mobility of the LPS/LPS-indol complex peak also indicated that an interaction was taking place. K_b values were produced by pooling the duplicates of each run to generate double, X-, and Y-reciprocal plots. The average of the three K_b values produced was 0.962 mg·L^{-1}. When converted to mol· L^{-1} by way of a conservative LPS mass estimate of 10-20 kDa, the result is a K_b range of 9.62- 19.2 x 10^6 L·mol^{-1}. This value is likely underestimated rather than overestimated given the conversion assumes a single LPS unit, while it is more likely in a micelle with a much larger mass. Use of a larger LPS mass would only increase the estimated K_b value. The X-reciprocal correlation coefficient was only 0.7807, which could be a preliminary indication that the stoichiometry of the binding is not 1:1 (13). In future, the X-reciprocal plot could be used to elucidate two K_bs; however a larger data set would be required (11). If future work is to follow the design of this study, more replicates need to be conducted to include upwards of seven LPS concentrations dissolved in the buffer and triplicates of each run to be performed. If a frontal analysis (FACE) study can be successfully designed and accomplished, it would eliminate both the limitations of stoichiometry and the unknown LPS mass (21). FACE is not limited to 1:1 binding stoichiometry and it would allow the indol concentration to be varied instead of that of LPS. FACE attempts for the interaction of indol and LPS are discussed in Chapter 4. Results generated using the traditional ACE method with LPS in the run buffer corroborate the current theory that LPS is the receptor for indol and that the equilibrium strongly favours complexation.

References

1. Selsted ME, Novotnytll MJ, Morris WL, Tang Y, Smith W, Cullor JS. Indolicidin, a novel bactericidal tridecapeptide amide from neutrophils. J Biol Chem. 1991;267(7):4292-5.

2. Peschel A, Sahl H. The co-evolution of host cationic antimicrobial peptides and microbial resistance. Nature Rev Microbiol. 2006 07;4(7):529-36.

3. Sader HS, Fedler KA, Rennie RP, Stevens S, Jones RN. Omiganan pentahydrochloride (MBI 226), a topical 12-amino-acid cationic peptide: Spectrum of antimicrobial activity and measurements of bactericidal activity. Antimicrob Agents Chemother. 2004 Aug;48(8):3112-8.

4. Bhargava A, Osusky M, Hancock RE, Forward BS, Kay WW, Misra S. Antiviral indolicidin variant peptides: Evaluation for broad-spectrum disease resistance in transgenic nicotiana tabacum. Plant Science. 2007 3;172(3):515-23.

5. Podorieszach AP, Huttunen-Hennelly H. The effects of tryptophan and hydrophobicity on the structure and bioactivity of novel indolicidin derivatives with promising pharmaceutical potential. Org Biomol Chem. 2010 04;8(7):1679-87.

6. Nagpal S, Kaur KJ, Jain D, Salunke DM. Plasticity in structure and interactions is critical for the action of indolicidin, an antibacterial peptide of innate immune origin. Protein Sci. 2002 Sep;11(9):2158-67.

7. Deeb SE, Wätzig H, El-Hady DA. Capillary electrophoresis to investigate biopharmaceuticals and pharmaceutically-relevant binding properties. TRAC Trend Anal Chem. 2013 0;48(0):112-31.

8. Dvorák M, Svobodová J, Benes M, Gas B. Applicability and limitations of affinity capillary electrophoresis and vacancy affinity capillary electrophoresis methods for determination of complexation constants. Electrophoresis. 2013;34(5):761-7.

9. Sekhon BS. An overview of capillary electrophoresis : Pharmaceutical , biopharmaceutical and biotechnology applications. J Pharm Educ. 2011;2(2).

10. El-Hady D, Kühne S, El-Maali N, Wätzig H. Precision in affinity capillary electrophoresis for drug–protein binding studies. J Pharm Biomed Anal. 2010 6/5;52(2):232-41.

11. Liu J, Hail M,E., Lee M,S., Abid S, Hangeland J, Zein N. Use of affinity capillary electrophoresis for the study of protein and drug interactions. Analyst. 1998;123(7):1455-9.

12. Tanaka Y, Terabe S. Estimation of binding constants by capillary electrophoresis. J Chromatogr B. 2002 02;768(1):81-92.

13. Bowser MT, Sternberg ED, Chen DD. Quantitative description of migration behavior of porphyrins based on the dynamic complexation model in a nonaqueous capillary electrophoresis system. Electrophoresis. 1997 Jan;18(1):82-91.

14. Hancock REW, Rozek A. Role of membranes in the activities of antimicrobial cationic peptides. FEMS Microbiol Lett. 2002;206(2):143-9.

15. El-Hady D, Kühne S, El-Maali N, Wätzig H. Precision in affinity capillary electrophoresis for drug–protein binding studies. J Pharm Biomed Anal. 2010 6/5;52(2):232-41.

16. Sigma- Aldrich. Lipopolysaccharides [Internet]; 2014. Accessed Jan 2015. Available from: http://www.sigmaaldrich.com/technical-documents/articles/biology/glycobiology/lipopolysaccharides.html

17. Fang N, Chen DDY. Behavior of interacting species in capillary electrophoresis described by mass transfer equation. Anal Chem. 2006;78(6):1832-40.

18. Jann B, Reske K, Jann K. Heterogeneity of lipopolysaccharides. Analysis of polysaccharide chain lengths by sodium dodecylsulfate-polyacrylamide gel electrophoresis. Eur J Biochem. 1975 Dec 1;60(1):239-46.

19. Yu L, Tan M, Ho B, Ding JL, Wohland T. Determination of critical micelle concentrations and aggregation numbers by fluorescence correlation spectroscopy: Aggregation of a lipopolysaccharide. Anal Chim Acta. 2006 Jan 18;556(1):216-25.

20. Sigma- Aldrich. Lipopolysaccharides from *Escherichia coli* O111:B4 product information [Internet]; 2013. Accessed Jan 2015. Available from: http://www.sigmaaldrich.com/content/dam/sigma-aldrich/docs/Sigma/Product_Information_Sheet/2/l2630pis.pdf

21. Busch MHA, Carels LB, Boelens HFM, Kraak JC, Poppe H. Comparison of five methods for the study of drug–protein binding in affinity capillary electrophoresis. J Chromatogr A. 1997 8/15;777(2):311-28.

CHAPTER 4: ROADS NOT FOLLOWED- FRONTAL ANALYSIS

Introduction

As with many research projects, this one began with a very specific goal of using frontal analysis capillary electrophoresis (FACE) to achieve a binding constant (K_b) for the interaction of indolicidin (indol) with lipopolysaccharide (LPS) followed by elucidation of the type of non-covalent interaction by way of a thermodynamic study. Attempts to accomplish this objective went on for many months before a new approach was taken to determining a K_b (see Chapters 2 & 3). Since space in journals is at a huge premium, it is simply not that common in science to report failures. While understandable, it is also a shame in many respects, as the attempts that do not work involve as much dedicated time in the laboratory as the attempts that result in fruitful publications. Without communicating these failures, what is to stop future researchers from wasting time on the same unproductive efforts? What follows is a brief description of why the FACE method was attempted, the study design, unfinished results and concluding remarks.

FACE is well regarded as a robust, simple, and reliable method for the determination of a K_b (1, 2). It is also a highly attractive method because it does not require the assumption of a 1:1 binding stoichiometry (3). For these reasons, the pursuit of a K_b was first attempted by optimizing a FA study. The experimental design involves injection of large "plugs" of sample. Rather than a standard short injection of 1-5 s producing peaks, FACE uses injection times upwards of 1-2 mins producing plateaus (Figure 4.1). Studies commence by optimizing CE parameters followed by building a calibration curve of free ligand plateaus of increasing height. The samples that are later injected are pre-equilibrated samples of constant concentration of analyte and increasing concentrations of ligand. The resulting

injection contains free analyte, free ligand and analyte-ligand complex. It is

assumed that the analyte and the complex will migrate at similar rates, but it is

required that the ligand have a sufficiently different mobility so that it leaks out of

the plug in a concentration proportional to the free ligand in the injected sample

(Figure 4.2)(1). The height of the free ligand portion of the plateau can then be

quantified by comparison to the standard curve. Finally, this data is used to plot the

number of complexed ligand molecules per molecule of analyte as a function of the

free ligand concentration (4). The resulting binding curve is fit using non-linear

regression.
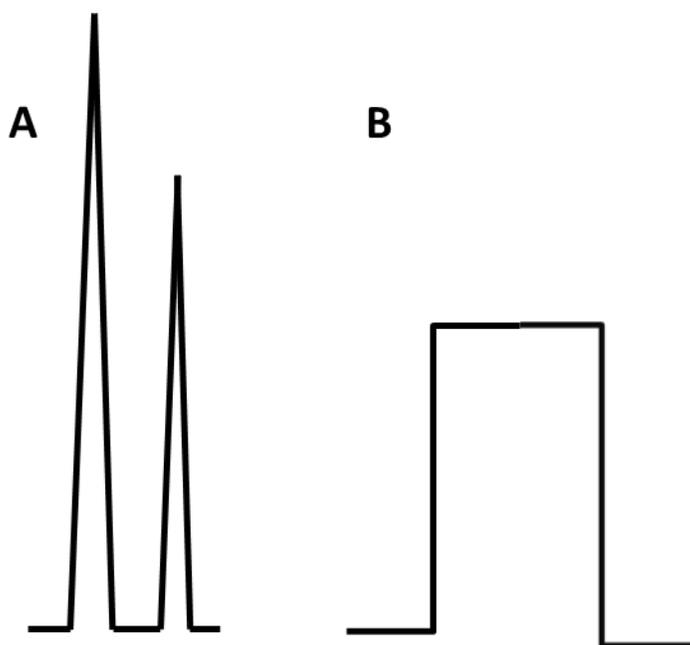
Figure 4.1: Representation of a short injection producing a peak (A) and a long injection (B) producing a plateau.
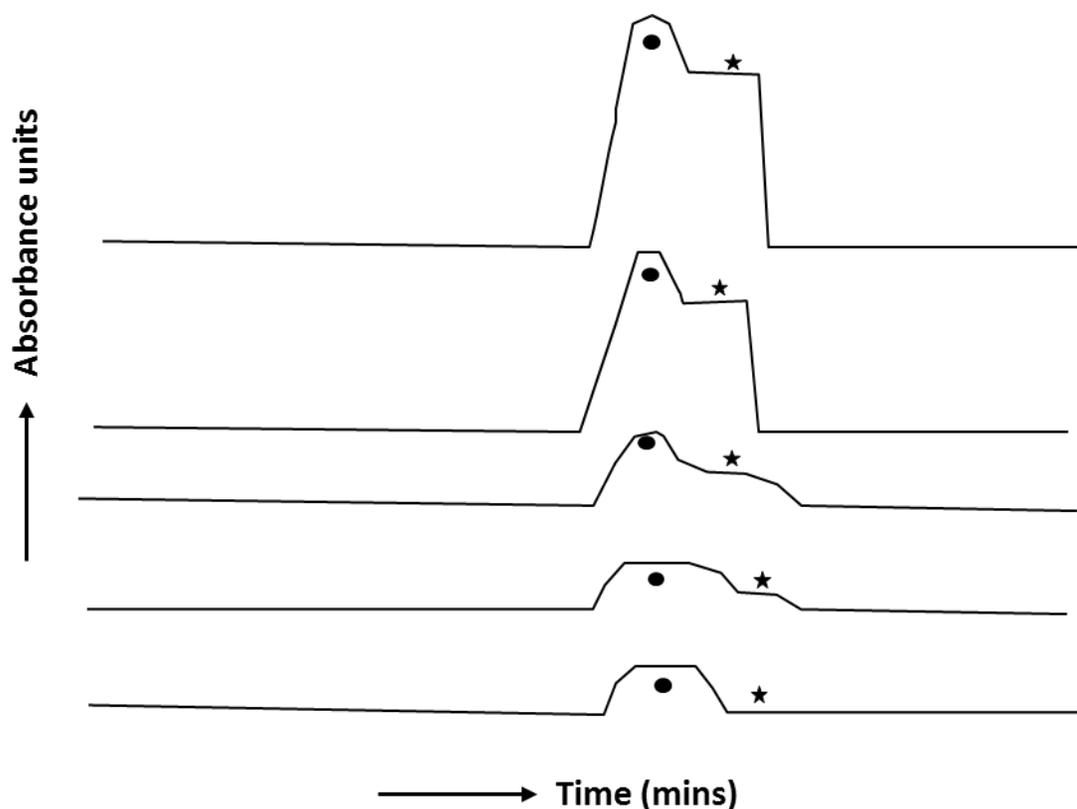
Figure 4.2: Theoretical representative electropherograms of a FACE study. ● is the analyte + the analyte-ligand complex. ★ is the free ligand.

Multiple attempts were made to allow use of FACE for elucidating a K_b for the interaction of indol with its proposed receptor- LPS (5). CE condition parameters were optimized to the physiological pH (~7.4) in order to give the results authority with respect to *in vivo* interactions. The following sections will summarize the experimental design for this study in a traditional manner, outlining the materials used, samples prepared, limited results, and discussion.

Experimental

Materials and reagents

All reagents used were of analytical-grade, and all reagents and background

electrolytes (BGEs) were filtered through 0.45-µm Nylon® syringe filters (Canadian

Life Science, ON, Canada). At this time, 0.45-µm Cellulose Acetate® were not yet in

use to help reduce protein loss due to adsorption, however, any protein loss would

be equivalent and represented throughout the samples as the same stock solutions

were used for all samples. Indolicidin (97.18% pure) was from GL Biochem Ltd. in

Shanghai, China and LPS isolated from *E.coli* (0111:B4) and monobasic sodium

phosphate ($NaH_2PO_4 \cdot H_2O$) were purchased from Sigma-Aldrich, Oakville, Ontario,

Canada. Caledon Laboratories in Georgetown, Ontario, Canada supplied the dibasic

sodium phosphate ($Na_2HPO_4 \cdot H_2O$). The water used to prepare all solutions was 18

MΩ water filtered by Barnstead™ Easypure™ RoDi.

BGE and Sample preparation

The desired pH of 7.2 (+/- 0.3) was ensured by the Mettler Toledo FE20 – FiveEasy™

pH meter. A 100 mM stock phosphate buffer was prepared by mixing 100 mM

dibasic sodium phosphate ($Na_2HPO_4 \cdot H_2O$) and 100 mM monobasic sodium

phosphate ($NaH_2PO_4 \cdot H_2O$) to a pH of 7.0. The 100 mM phosphate buffer was then

diluted 10-fold to make a 10 mM phosphate buffer which was stored at room

temperature (~23°C) and used for no more than 30 days.

LPS of 520 mg·L^{-1} was prepared by dissolving directly into the 10 mM

phosphate buffer. Indol was prepared by dissolving directly into the 10 mM

phosphate buffer (pH 7.0) to a final concentration of 640 mg·L^{-1}. The solutions were

stored in the refrigerator (~4°C) and used for a maximum of 30 days. All stocks and reagents were filtered using 0.45-μm Nylon® filters prior to injection into CE. Calibration curves were desired for both LPS and indol so that the size and shape of electropherograms of each could be optimized. LPS samples were made in increasing concentrations from 130 mg·L^{-1} to 303 mg·L^{-1} (molar equivalent unknown). Indol samples were made in the range of 78 mg·L^{-1} to 401 mg·L^{-1} (equivalent of 41 μM to 210 μM).

Apparatus

Data was collected using a Beckman Coulter ProteomeLab™ PA 800 capillary electrophoresis instrument with detection at 214 nm with an ultraviolet (UV) detector set at direct absorbance. A fused-silica capillary from Polymicro Technologies, Phoenix, AZ, USA, of outer diameter 366.0 ± 0.2 μm, inner diameter 50.4 ± 0.2 μm, 40 cm effective length (to detector) and 50 cm total length was used. A circulating liquid fluorocarbon coolant allowed the temperature in the capillary cartridge to be maintained at 25 °C. Normal polarity was used for all runs with voltage set at 10 kV for 20-30 mins- enough time to observe all expected plateaus.

New capillaries were conditioned (each at 20 psi) with 1.0 M NaOH for 60 min, followed by 0.1 M NaOH for 30 min. Before the sequence was started, the capillary was flushed (each for 10 mins at 20 psi of pressure) with H$_2$O, 0.1 M NaOH, H$_2$O, and plain 100 mM phosphate buffer (pH 7.3). Prior to each sample injection, the capillary was flushed (each at 20 psi) with 0.1 M NaOH for 14 min, H$_2$O for 2 min, and then phosphate buffer for 4 min. Extensive use of rinse steps is always recommended to reduce protein adsorption to the uncoated capillary (6). In this

study, introduction of a large plug of cationic indol made the need for rinsing increasingly important- thus the NaOH rinse was increased from the standard pre-run rinse time of 4 mins to 14 mins. Each sample was injected (as a rinse parameter) for the optimized "plateau-producing" 120 s at 1.0 psi. Gentle vortexing ensured that each sample was well mixed. All runs were produced in triplicate. Following completion of reasonable calibration curves for each of indol and LPS, pre-incubated samples within similar concentration ranges were attempted by primarily varying the indol concentration and keeping the LPS concentration constant.

Results and Discussion

Optimizing LPS plateaus

LPS was quite easy to optimize. The overall neutral properties of LPS lend themselves to beautiful plateaus when samples are subjected to long injection. Figure 4.3 shows plateaus of increasing height generated from the LPS concentration range of 130 mg·L^{-1} to 303 mg·L^{-1}. Triplicates of these samples were run, each having very similar appearances. The increasing plateau height is evident with increasing concentrations of LPS. The purpose of the LPS plateaus is primarily to observe the shape and size of the resulting electropherograms for optimization and was conducted successfully.
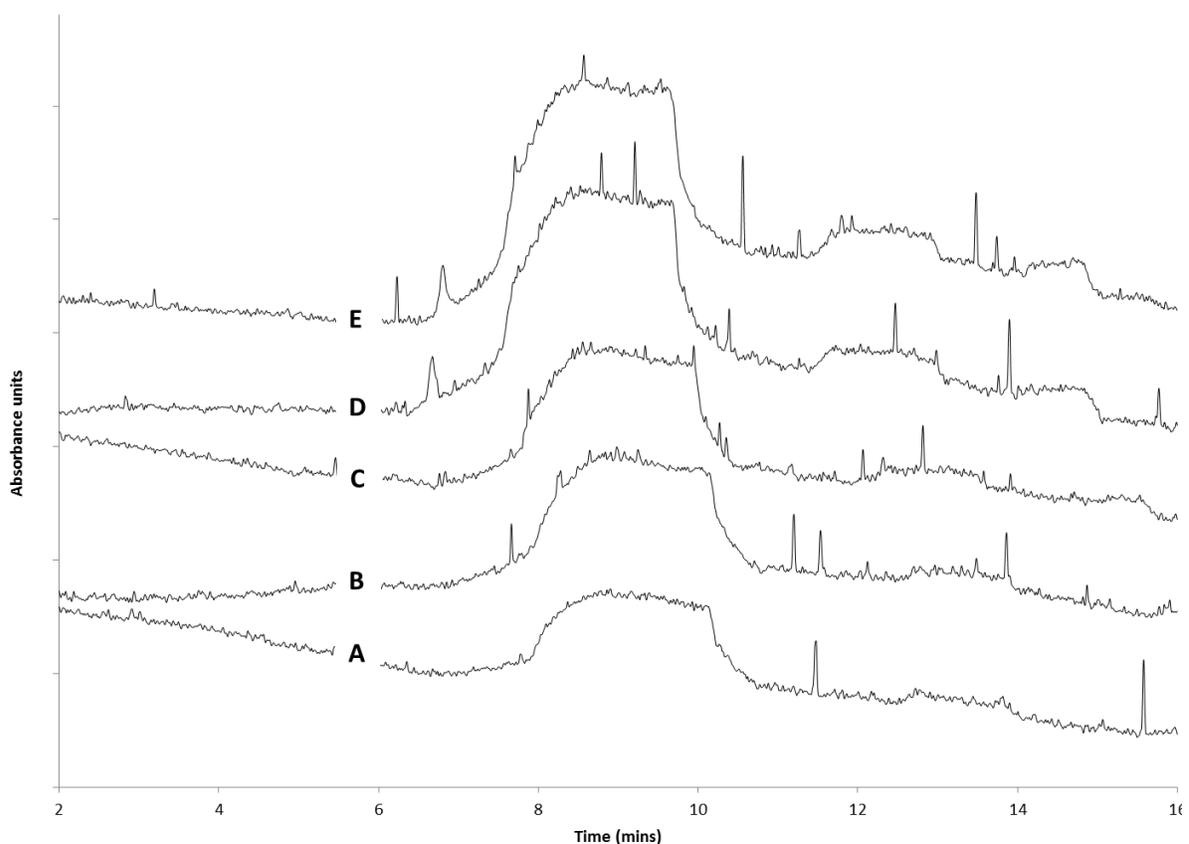
Figure 4.3: Representative electropherograms of samples of LPS mixed to varying concentration in 10 mM phosphate buffer (pH 7.0). LPS concentrations were A) 130, B) 173, C) 217, D) 260, and E) 303 mg·L^{-1}. CE conditions are described in the Apparatus section.

Indolicidin Standard Curve

After reproducible injection parameters were determined for LPS, an indol standard curve was then attempted using the same parameters. The study as a whole requires development of an indol standard curve so that the LPS can remain constant and indol can be varied when pre-incubation and plug injection take place. This is necessary because indol is the drug and its free fraction will migrate at a significantly different rate than the LPS/LPS-indol fraction due to size and charge. It is then also helpful that the molecular mass of indol is known (1.9063 kg·mol^{-1})

while LPS's is not (Sigma Aldrich reports a mass range of 10-20 kg·mol^{-1}) (7).

Unfortunately, a standard curve for indol is harder to build. The cationic nature of indol causes adsorption to the silanol groups of the inner wall of the capillary, especially to surface defects (8). The result is plateaus with a less desirable shape that strays from that of an ordinary plateau (Figure 4.4). Reducing the pH to 5 or 6 would alleviate this issue, but would result in findings that are not applicable to physiological systems. Capillary coatings were also briefly attempted (cationic PB-DS-PB and neutral CHO carbohydrate coating), however, results continued to be unfavourable and a bare fused silica capillary was reinstated. Best efforts were made to build a standard curve for indol at the physiological pH. All runs were performed in triplicate, with each replicate appearing very similar. As indol concentration is increased, more cationic peptides are available for adsorption, and a peak is seen to appear within the indol plateaus (most visible on Figure 4.4 **C** & **D**). It is assumed that this peak is generated by large volumes of indol being released from their attractions to the inner walls and migrating to the detector in large groups. After many attempts to better optimize the BGE solution and its concentration, voltage, ligand concentration, injection time and pressure, to no avail, it was finally decided to move on with the calibration curve pictured in Figure 4.4 Moving forward would at least give a feel for whether FACE could be a viable method after all.
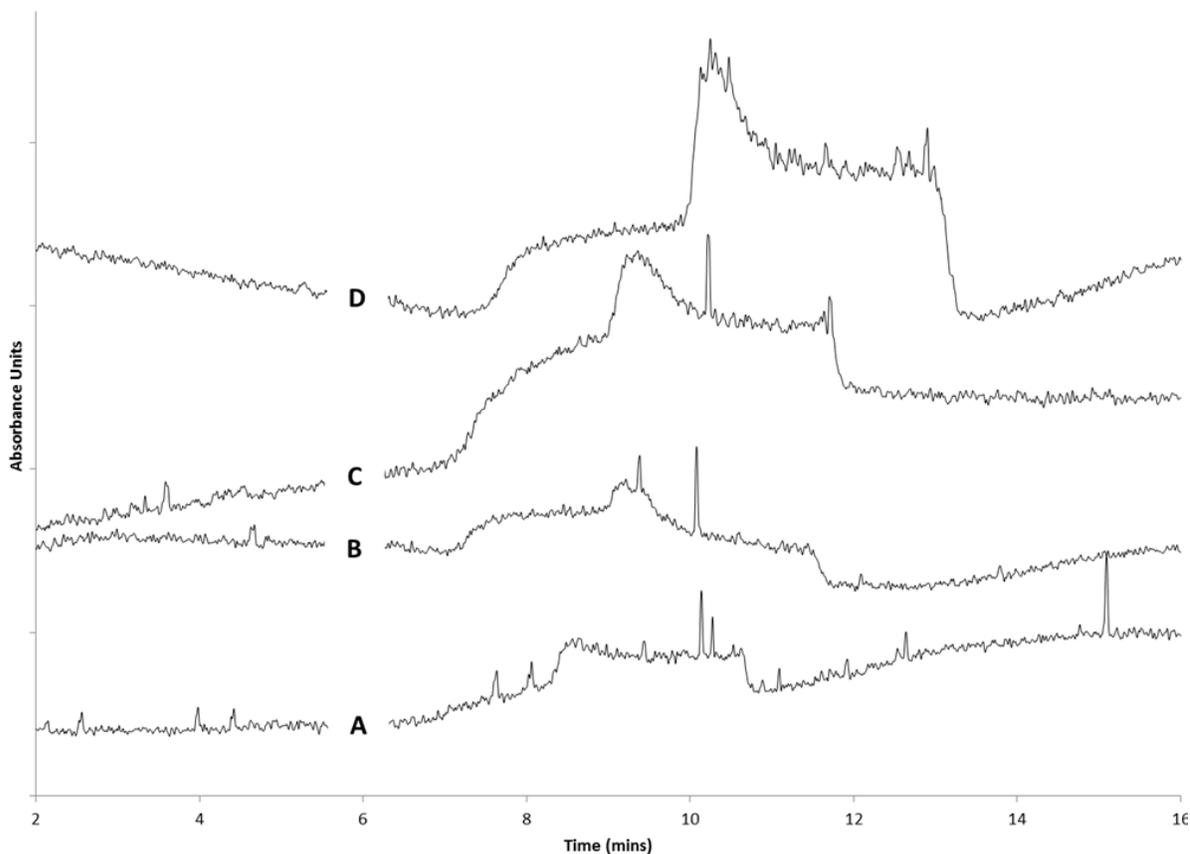
Figure 4.4: Representative electropherograms of varying concentrations of indol in 10 mM phosphate buffer (pH 7.0). Indol concentrations were A) 79, B) 175, C) 217, D) 300 mg·L^{-1}. CE conditions are described in the *Apparatus* section.

Attempting FACE

Once an indol standard curve was built, we could proceed to combine our drug with our receptor, in this case indol with LPS. The concentration of indol is varied while that of LPS is kept constant. Incubation time of the samples could play an important role in the final calculated K_b value. To get an idea of the effects of incubation time, triplicate runs of each sample are conducted consecutively, resulting in incubation time of approximately 1 hr, 2.5 hrs and 4hrs. The goal is to assess the changes that

occur at these incubation times and to see if and when the equilibrium seems to be reached. Since the concentration ranges used for both the free indol and LPS were in the range of 50-400 mg·L^{-1}, the first set of pre-incubated samples were made with a constant 250 mg·L^{-1} of LPS and 100, 175 and 250 mg·L^{-1} indol (Figure 4.5).

As can be seen by Figure 4.5, there is a shoulder on each of the electropherograms, which does seem to indicate an increase in the proportion of free indol. The triplicates of each sample were very similar in migration time and overall plateau shape indicating that equilibrium is in fact already established at 1 h and little change is experienced thereafter. Based on the shape of these preliminary outputs, the next samples were run with lower concentrations in an attempt to reduce the overall plateau height (Figure 4.6).
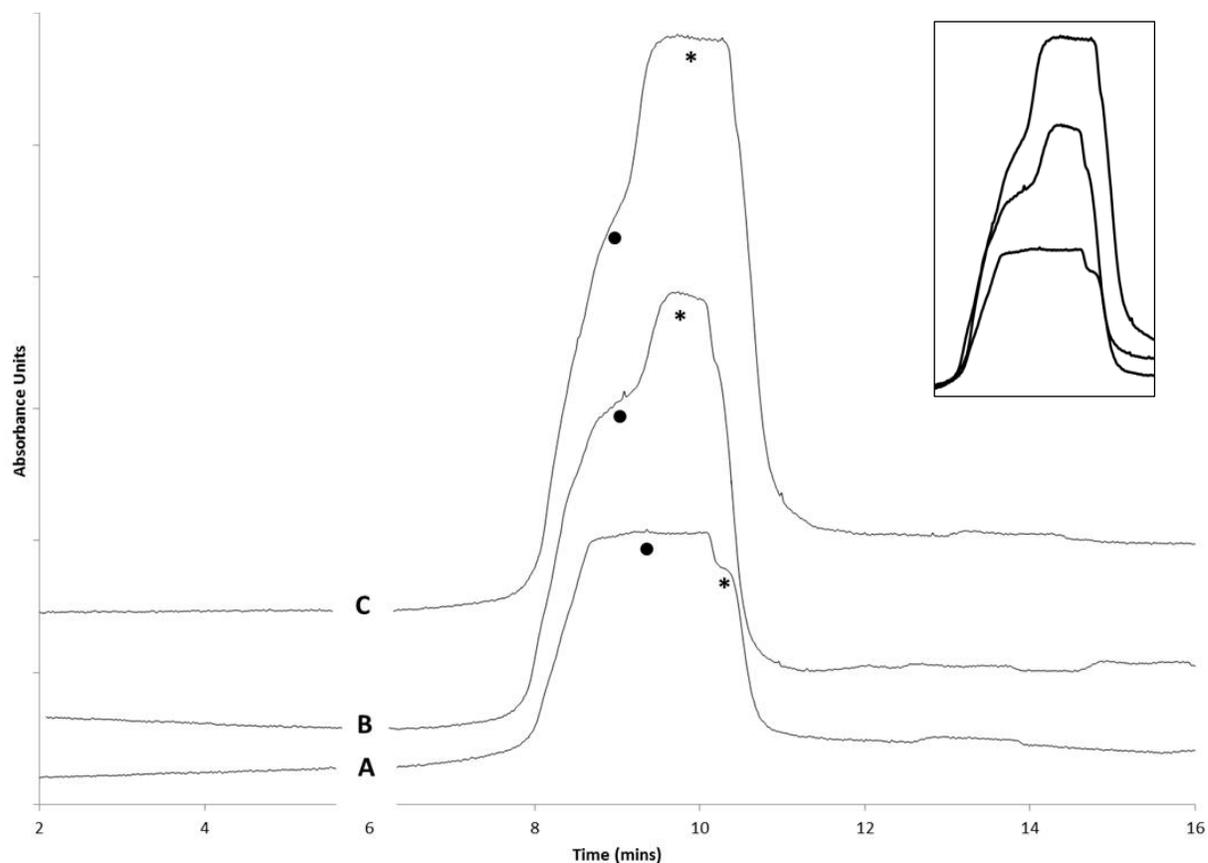
Figure 4.5: First electropherograms from the pre-incubation of varying concentrations of indol with constant 250 mg·L⁻¹ concentration of LPS. Indol concentrations were A) 100, B) 175, and C) 250 mg·L⁻¹. ● is the LPS/LPS-indol complex, and * is the free indol. CE conditions are described in the *Apparatus* section. Incubation times varied from 1-4 hours.
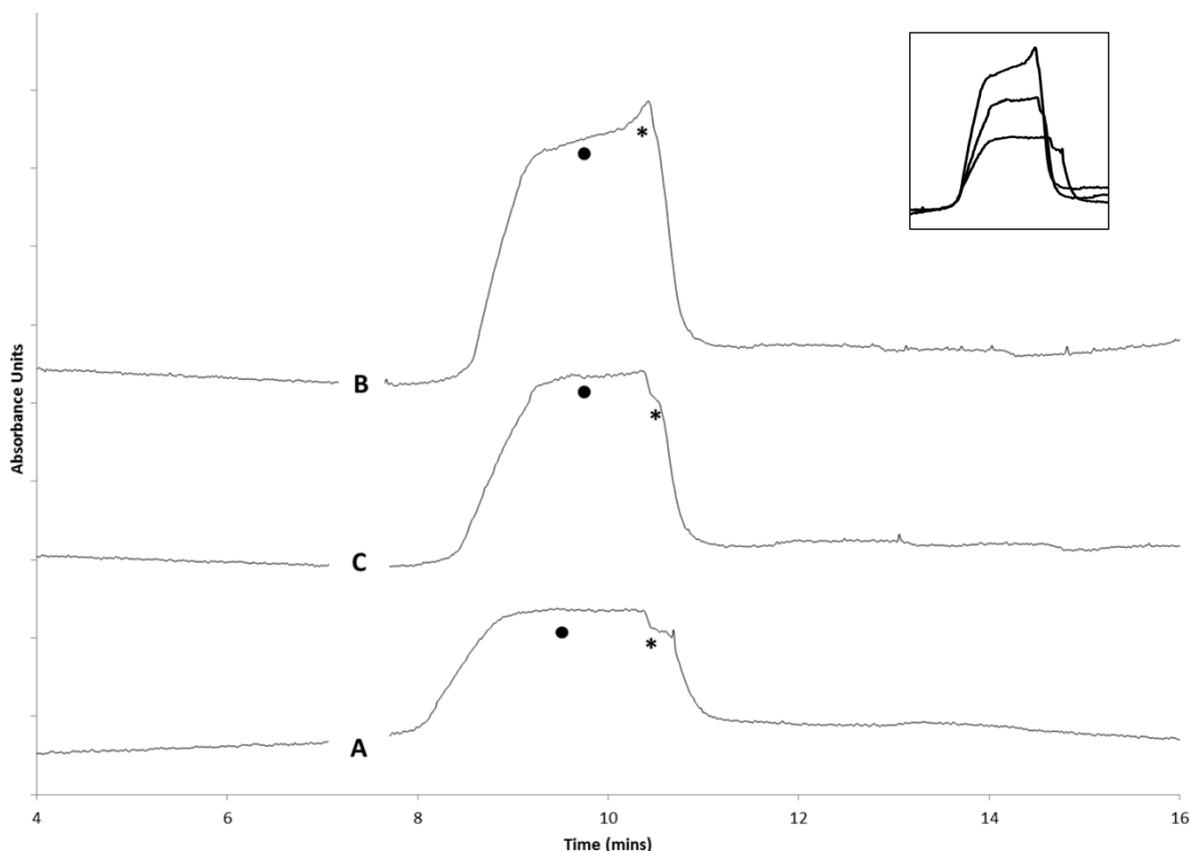
Figure 4.6: Pre-incubation of varying concentrations of indol with constant 150 mg·L⁻¹ concentration of LPS. Indol concentrations were A) 50, B) 87.5, and C) 125 mg·L⁻¹. ● is the LPS/LPS-indol complex, and * is the free indol. CE conditions are described in the *Apparatus* section. Incubation times varied from 1-4 hours.

The trends of increasing free indol fraction are consistent at both the higher and the lower concentration ranges as seen in Figures 4.5 and 4.6, respectively. To definitively indicate the identity of the shoulder, spiking was conducted where 350 mg·L⁻¹ of indol was mixed with just 130 mg·L⁻¹ LPS. The outcome was a very sharp increase in the height of the indol portion of the resulting plateau in the region where it was expected (on the righter-most side of the plateau) (Figure 4.7). With a definitive trend identified and corroboration of the region of the plateau that represents the free indol fraction, consideration was then given to the concentrations

that should ultimately be used for further analysis. Upon overlaying the pre-incubated electropherograms with those of free indol and LPS of similar concentrations, it becomes apparent that there is an absorbance issue (Figure 4.8). The plateau heights produced from mixing the LPS and the indol dwarf the plateaus of both free indol and LPS of similar concentrations produced under the same CE conditions, but on separate days. The free indol and LPS analyses were performed four days prior to the analysis of mixed indol/LPS.   In order to be able to use the indol calibration curve for interpolation, the height of the resulting indol fraction needs to be within the calibration range.

In the second round of FACE attempts (Figure 4.6), the concentrations of indol that were mixed with LPS $\leq$ to 125 mg·L^{-1} and yet based on the indol calibration curve, the fraction of free indol is outside the range of the reference standards which were in the range of 79 mg·L^{-1} to 324 mg·L^{-1}. An explanation for the sudden absorbance increase is not forthcoming. It could only be assumed that an unknown change occurred to the instrument between data collections.
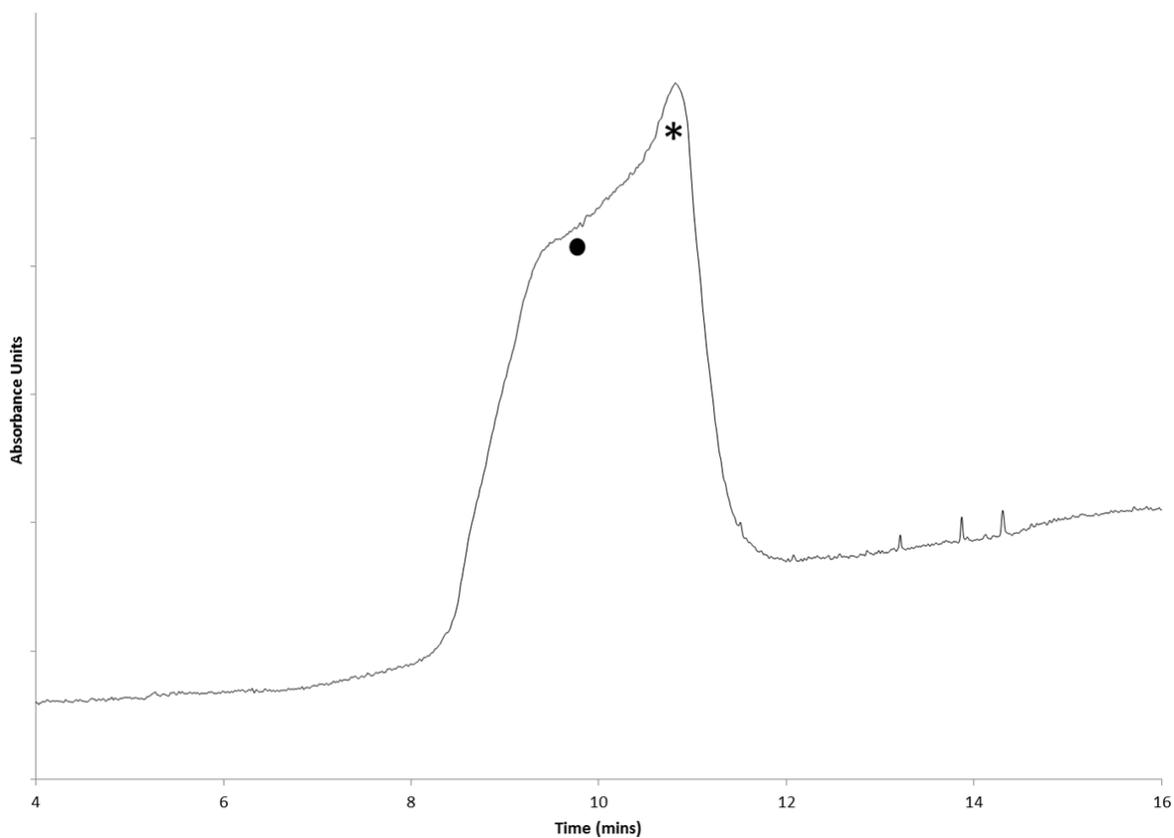
Figure 4.7: Pre-incubation of 130 mg·L⁻¹ LPS with 350 mg·L⁻¹ indol to identify the righter-most region of the plateau as free indol. ● is the LPS/LPS-indol complex, and * is the free indol. CE conditions are described in the Apparatus section. Incubation times varied from 1-4 hours.
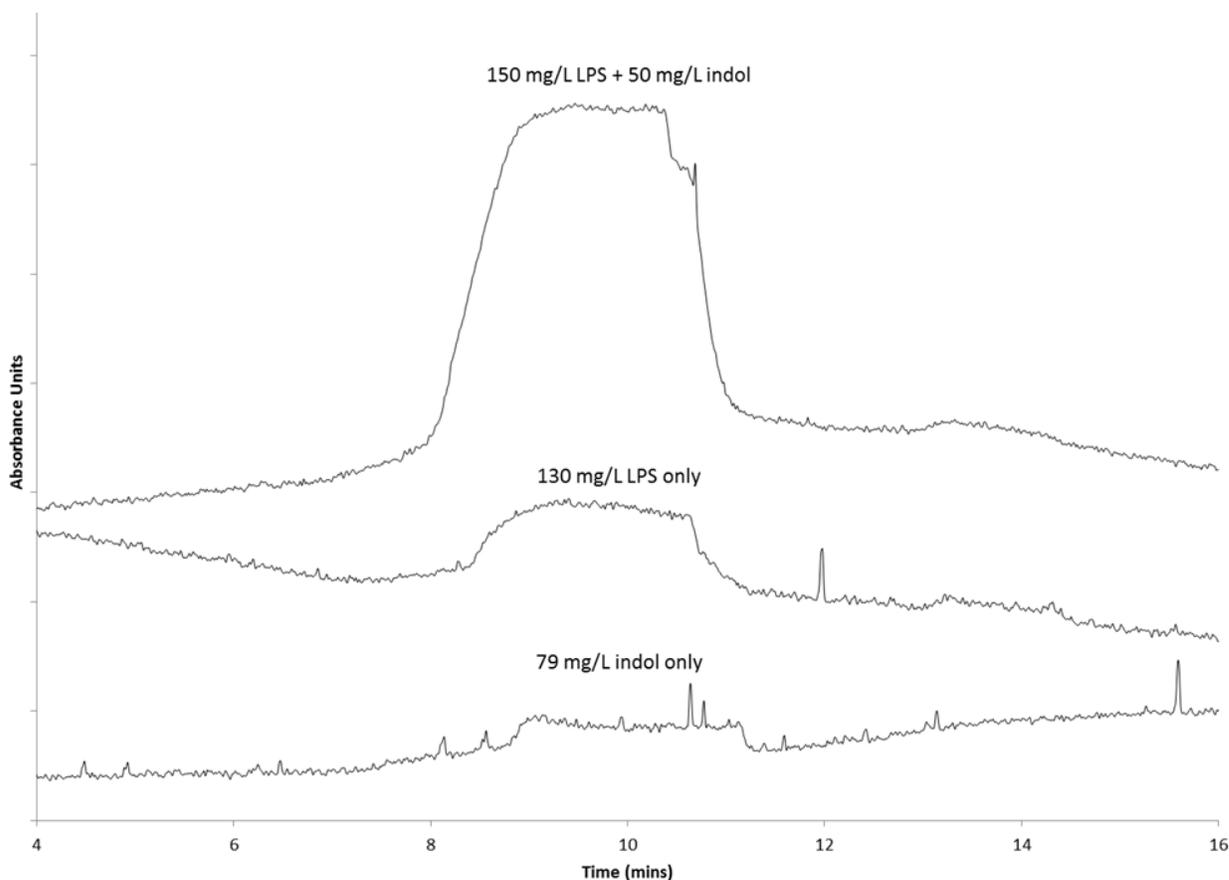
Figure 4.8: Overlay of the 150 mg·L^{-1} LPS mixed with 50 mg·L^{-1} indol electropherogram with free LPS and indol electropherograms (130 mg·L^{-1} and 79 mg·L^{-1}, respectively). CE conditions are described in the Apparatus section. The x and y axis were altered for ease of comparison.

Conclusion

The electropherograms produced from mixing LPS and indol were considered unusable because the shoulder that we have now identified as the free indol fraction was not recognized. Once the free indol portion of the plateaus was identified and the data was further investigated, it was discovered that mixing indol and LPS somehow increased absorbance by the complex and the values for free indol fall

outside the range of the calibration curve. This work was set aside before completion due to adsorption troubles faced when building the indol standard curve, a misunderstanding of the mixed sample plateau outputs and finally a mismatch of absorbance readings. If this work is to be attempted again in the future, optimizing a shorter injection time (*ie*., 30-60s) might result in less adsorption when building the indol calibration curve. Most importantly, to save precious time, run indol by itself and then immediately, within the same sequence, compare the absorbance readings of the free indol analysis with absorbance readings of indol mixed with LPS. With any luck, the absorbance changes that were seen in the results herein were from an unidentified change to the instrument and will not cause similar confusion in future research.

References

1. Busch MHA, Carels LB, Boelens HFM, Kraak JC, Poppe H. Comparison of five methods for the study of drug–protein binding in affinity capillary electrophoresis. J Chromatogr A. 1997 8/15;777(2):311-28.

2. Østergaard J, Hansen SH, Jensen H, Thomsen AE. Pre-equilibrium capillary zone electrophoresis or frontal analysis: Advantages of plateau peak conditions in affinity capillary electrophoresis. Electrophoresis. 2005 Nov;26(21):4050-4.

3. Hancock RE, Sahl HG. Antimicrobial and host-defense peptides as new anti-infective therapeutic strategies. Nat Biotechnol. 2006 Dec;24(12):1551-7.

4. Østergaard J, Heegaard NHH. Capillary electrophoresis frontal analysis: Principles and applications for the study of drug-plasma protein binding. Electrophoresis. 2003 09;24(17):2903-13.

5. Nagpal S, Kaur KJ, Jain D, Salunke DM. Plasticity in structure and interactions is critical for the action of indolicidin, an antibacterial peptide of innate immune origin. Protein Sci. 2002 Sep;11(9):2158-67.

6. El-Hady D, Kühne S, El-Maali N, Wätzig H. Precision in affinity capillary electrophoresis for drug–protein binding studies. J Pharm Biomed Anal. 2010 6/5;52(2):232-41.

7. Sigma- Aldrich. Lipopolysaccharides [Internet]; 2014. Accessed Jan 2015. Available from: http://www.sigmaaldrich.com/technical-documents/articles/biology/glycobiology/lipopolysaccharides.html

8. Kaupp S, Steffen R, Wätzig H. Characterisation of inner surface and adsorption phenomena in fused-silica capillary electrophoresis capillaries. J Chromatogr A. 1996 9/13;744(1–2):93-101.

CHAPTER 5: CONCLUSION

Motivation for novel drug discovery is global and the growing crisis in antibiotics is being broadcast on mainstream news networks regularly. The introduction of a novel antibiotic could allow us a fresh start: a drug that is used in appropriate doses, and for appropriate applications. The process of drug development is long and arduous and requires many different steps in research development. Each and every drug-related study contributes to the body of knowledge that could expedite the process of getting the latest discovery to market. Cationic antimicrobial peptides (CAPs) have been the focus of extensive research due to their broad potential for use. While an astounding break-through is still to come, adding to the knowledge and tools available for drug study could contribute to that much needed break-through. The CAP indolicidin (indol) is unlikely to be the precise revolutionary drug that helps to curb antibiotic resistance; however, the methods that are developed for its study can further be applied to other possibilities and gets us closer to a solution to the ever growing problem of antibiotic resistance. The variations of indol that have been developed are excellent candidates for continued study (1-3). The methods for studying indol with capillary electrophoresis (CE) optimized within this thesis are very likely applicable to studying those mutants.

Determining a preliminary binding constant (K_b) between a drug and its receptor is an important step in beginning drug discovery (4). This thesis can be viewed as a road-map for how best to study the indol-lipopolysaccharide (LPS) interaction. Frontal Analysis (FA) CE was the least optimized method reviewed, however it has the greatest promise when it comes to elucidating a K_b that can indicate multiple

binding. Research using the FA study design was originally halted due to the perception of poor results. That perception has since been reconsidered, and the prospect of continuing research with FA parameters is optimistic. For a researcher attempting to continue this work, the optimized conditions for producing well-resolved electropherograms are provided with suggestions for improvement in Chapter 4.

Affinity CE (ACE) and pre-incubation ACE (PI-ACE) were also discussed within this thesis in Chapters 3 and 2, respectively. For the traditional ACE method, a K_b range was determined as 9.62- 19.2 x 10^6 L·mol^{-1}. The range is limited by the assumption of the LPS molecular mass, which was assumed to be 10-20 kDa (5). Determining a precise K_b while adding LPS as a run buffer additive is going to introduce error due to the ambiguity of the LPS mass, however, given that the LPS used (from *E.coli* 0111:B4- Sigma Aldrich) forms aggregates of 43-49 molecules per micelle, we can be quite confident that the reported K_b range of 9.62- 19.2 x 10^6 L·mol^{-1} is underestimated rather than overestimated (6). Replication of this work with more LPS concentrations in the buffer and conducted in triplicate will greatly increase the confidence in the final reported K_b.

For the PI-ACE method, K_b values were produced for each of three incubation times that were investigated from the average of the three regression plots (double, X-, and Y-reciprocals). The values obtained were 5.22 x 10^5, 3.18 x 10^5, and 1.11 x 10^5 L·mol^{-1} for 2, 5.5 and 10 h ($\pm$ 0.5) incubations, respectively. A steady decrease in K_b was seen over the course of the incubation times studied and further investigation indicated that equilibrium appears to be established after approximately six hours of incubation. The values reported from the PI-ACE method suffer from very limited quantities of data. While the study design has been optimized and could be

reproduced in triplicate to give more confident results, the time required to analyze pre-incubated samples in a time-sensitive manner is excessive and this method would not be recommended as the most suitable option for K_b determination.

From the work that has been presented here, it is the author's hope that research will continue and result in publication of a confident K_b by using one or more of ACE as discussed in Chapter 3, PI-ACE as discussed in Chapter 2, or FACE as discussed in Chapter 4. These study designs can then be replicated to elucidate a K_b for the indol derivative known as Δ *4,5* which has shown heightened antimicrobial action and reduced cytotoxicity (1). Furthermore, LPS which has been used as the assumed Gram-negative cell receptor could then be replaced with sphingomyelin. Sphingomyelins are sphingolipids present in the plasma membrane of animal cells (7). They are thought to be the indol receptor in animal cells and a K_b between them could shed light on the mechanism of action and be helpful for further reducing cytotoxicity of indol mutants. Preliminary findings presented in this thesis corroborate the current belief that when indol interacts with a Gram-negative bacterial cell, LPS is its primary receptor.

The bigger picture

While antibiotic use and misuse is presenting a global health concern, is it also an environmental concern (8). Antibiotic resistance genes (ARGs), most commonly thought to be found in hospital settings, are being found in increasing quantities in the environment as well (9). Urban and agricultural environments are showing significant levels of ARGs in both the influent and effluent of wastewater and drinking water treatment plants (10-12). The presence of both ARGs and antibiotics

in our ecosystems is detrimental to the species within them. Many studies have endeavoured to quantify the extent of the hormones and drugs in our wastewater and the impact of the presence of those drugs (13, 14). For years, we have used a variety of over-the counter and prescription drugs for a variety of health-related reasons, not realizing their effect on a wide range of organisms in the environment and the resounding effect on environmental health (15). Misuse of antibiotics has led us to a reduction in ecosystem health and to the health crisis that is antibiotic resistance. Insufficient regulations and control surrounding antibiotics could literally mean a return to the pre-antibiotic era for many types of infections (16). The successful development of a new class of antibiotics at a time when we better understand the breadth of the mistakes we have made could allow us a second chance to get it right. While the need to develop new treatments is becoming more critical each day, the delay is exacerbating the importance of correctly managing any new discoveries so that we don't end up on this very same road just a decade or two from now.

References

1. Podorieszach AP, Huttunen-Hennelly H. The effects of tryptophan and hydrophobicity on the structure and bioactivity of novel indolicidin derivatives with promising pharmaceutical potential. Org Biomol Chem. 2010 04;8(7):1679-87.

2. Bhargava A, Osusky M, Hancock RE, Forward BS, Kay WW, Misra S. Antiviral indolicidin variant peptides: Evaluation for broad-spectrum disease resistance in transgenic nicotiana tabacum. Plant Science. 2007 3;172(3):515-23.

3. Sader HS, Fedler KA, Rennie RP, Stevens S, Jones RN. Omiganan pentahydrochloride (MBI 226), a topical 12-amino-acid cationic peptide:

Spectrum of antimicrobial activity and measurements of bactericidal activity. Antimicrob Agents Chemother. 2004 Aug;48(8):3112-8.

4. Tanaka Y, Terabe S. Estimation of binding constants by capillary electrophoresis. J Chromatogr B. 2002 02;768(1):81-92.

5. Sigma- Aldrich. Lipopolysaccharides [Internet]; 2014. Accessed Jan 2015. Available from: http://www.sigmaaldrich.com/technical-documents/articles/biology/glycobiology/lipopolysaccharides.html

6. Yu L, Tan M, Ho B, Ding JL, Wohland T. Determination of critical micelle concentrations and aggregation numbers by fluorescence correlation spectroscopy: Aggregation of a lipopolysaccharide. Anal Chim Acta. 2006 Jan 18;556(1):216-25.

7. Nelson D, Cox M. Lehninger principles of biochemistry. Fourth ed. New York, NY: Sara Tenney; 2005.

8. Levy SB, Marshall B. Antibacterial resistance worldwide: Causes, challenges and responses. Nat Med. 2004;10(12):S122-9.

9. Childress H, Sullivan B, Kaur J, Karthikeyan R. Effects of ultraviolet light disinfection on tetracycline- resistant bacteria in wastewater effluents. J Water Health. 2014:404-10.

10. Pei R, Kim SC, Carlson KH, Pruden A. Effect of river landscape on the sediment concentrations of antibiotics and corresponding antibiotic resistance genes (ARG). Water Res. 2006 Jul;40(12):2427-35.

11. Pruden A, Pei R, Storteboom H, Carlson KH. Antibiotic resistance genes as emerging contaminants: Studies in northern colorado. Environ Sci Technol. 2006 Dec 1;40(23):7445-50.

12. Chee-Sanford JC, Aminov RI, Krapac IJ, Garrigues-Jeanjean N, Mackie RI. Occurrence and diversity of tetracycline resistance genes in lagoons and groundwater underlying two swine production facilities. Appl Environ Microbiol. 2001 Apr;67(4):1494-502.

13. Chen Y, Yu G, Cao Q, Zhang H, Lin Q, Hong Y. Occurrence and environmental implications of pharmaceuticals in chinese municipal sewage sludge. Chemosphere. 2013 Nov;93(9):1765-72.

14. Plosz BG, Leknes H, Liltved H, Thomas KV. Diurnal variations in the occurrence and the fate of hormones and antibiotics in activated sludge wastewater treatment in oslo, norway. Sci Total Environ. 2010 Mar 15;408(8):1915-24.

15. Boxall ABA. The environmental side effects of medication. EMBO Rep. 2004 12;5(12):1110-6.

16. Spellberg B, Guidos R, Gilbert D, Bradley J, Boucher HW, Scheld WM, et al. The epidemic of antibiotic-resistant infections: A call to action for the medical community from the infectious diseases society of america. Clin Infect Dis. 2008;46:155-64.

APPENDIX A: AFFINITY CE WITH LPS AS THE SAMPLE AND INDOL DISSOLVED IN THE BACKGROUND ELECTROLYTE
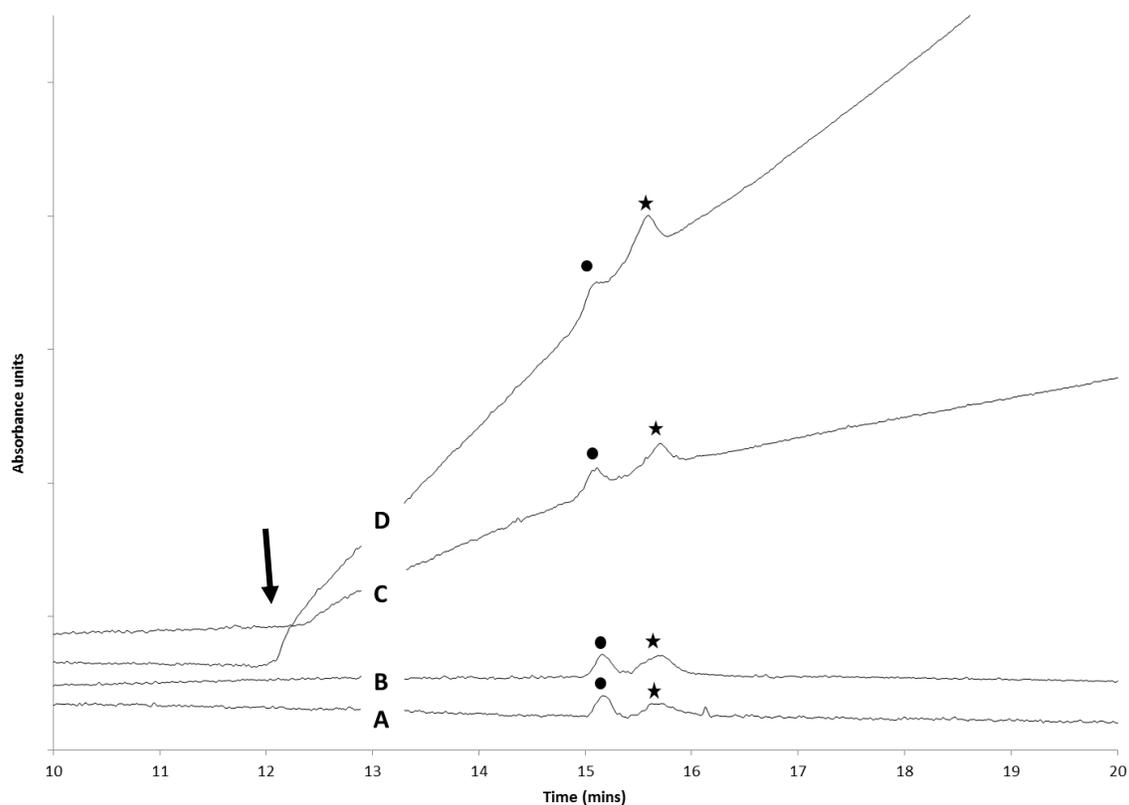
Figure A1: Representative electropherograms from the traditional ACE attempts with indol dissolved in the background electrolyte. Sample was a constant concentration of 50 mg·L⁻¹ LPS dissolved in 100 mM phosphate buffer (pH 7.3). Separation buffer was 100mM phosphate buffer (pH 7.3) with increasing concentrations of indol. Indol concentrations dissolved in run buffer were A) 0, B) 10, C) 20, and D) 50 mg·L⁻¹. ● is the DMSO neutral marker which was verified by spiking, and ★ is the LPS/LPS-indol complex.   The arrow indicates the time when a free indol sample peak would normally be present and shows where adsorption is very clearly occurring. Samples were injected for 5 s duration at 1.0 psi, with 10 kV separation voltage, normal polarity, detection at 214 nm, with 10 mM PO₄²⁻ (pH 7.3) as run buffer.

APPENDIX B: SOLID PHASE PEPTIDE SYNTHESIS OF INDOLICIDIN

Introduction

The antimicrobial peptide (AMP) indolicidin (indol) is a short sequence made of just 13 amino acids. Despite the small number of amino acids that make up its structure, it is still an expensive item to order in its purified form. Purchased from GenWay Biotech in San Diego, California, a 20 mg vial of >95% pure indol costs upwards of $500.00. In addition, the purified product can take 3-6 weeks to arrive to the lab for use. These factors render it advantageous to synthesize peptide sequences in-house. While an in-house synthesized indolicidin sample was not used for the research conducted herein, the process of producing indolicidin was started in the hopes of providing an ample supply for future research. What follows is a very brief overview of the steps involved to accomplish basic peptide synthesis. Subsequently, experimental use of the Tribute Peptide Synthesizer by Protein Technologies Inc, and the steps remaining to complete cleaving the peptide from the resin and of its side chain protecting groups and purification are presented.

Peptide Synthesis

Interest in peptide synthesis has been largely driven by the desire to discover novel drugs for therapeutic use. Synthesis of peptides by manipulation of amino acid sequences has allowed researchers to alter and improve the therapeutic properties of known peptides (1). Structures of natural products present an excellent starting point for synthesis of peptide sequences and can be improved upon by changes in

specific amino acids in a series. It is then also possible for non-natural amino acids to be used to further expand synthetic options (2).

The synthesis of peptides was revolutionized in 1963 by Robert Bruce Merrifield with the release of his journal article publication "Solid Phase Peptide Synthesis. I. The Synthesis of a Tetrapeptide"(3). At the time, liquid phase peptide synthesis was the method of choice and allowed for the easy synthesis of most small peptides. Merrifield's innovation of the solid phase method of peptide synthesis (SPPS) was able to overcome some of the challenges of solubility and purification problems faced when attempting larger peptide sequences. SPPS has since grown to become the preferred method, allowing for rapid synthesis of long peptides, automation, and a large capacity (4).

Peptide synthesis, in its simplest form, involves the joining of amino acids via peptide bonds. In SPPS, resins are used which provide a solid starting point, or scaffold on which the peptide sequence is built. Whether liquid or solid phase, the process consists of four general steps: 1) N protection, 2) OH activation, 3) Deprotection, and 4) Coupling. Each of these steps will be examined with respect to coupling of the first two amino acids of the indol sequence (Figure B1). In nature, protein synthesis is accomplished from the N terminus to the C terminus and thus the typical convention for writing an AA sequence is from N → C. In SPPS, the amino acids are coupled in reverse order, from the C terminus to the N terminus. In this particular scenario, the first amino acid to be added to the resin will therefore be arginine (R), followed by another arginine (R), and then tryptophan (W) and so on. To understand the overall process of SPPS, it is important to first grasp the concepts of N protection and OH activation.

N → C	C → N
I-L-P-W-K-W-P-W-W-P-W-R-R	R-R-W-P-W-W-P-W-K-W-P-L-I

Figure B1: Indolicidin amino acid sequence depicted from N to C terminus and C to N terminus.

N protection

Without the use of N protection, several combinations of coupling are possible between two amino acids as multiple nitrogen groups would be available to react. By using the steps of 1) N protection and 2) OH activation, the direction of the reaction can be greatly controlled resulting in a higher percentage of the desired peptide sequence.   Reaction 1 depicts protection of one nitrogen on arginine with a very common protecting group, fluorenylmethyloxycarbonyl chloride (Fmoc).

Fluorenylmethyloxycarbonyl chloride (Fmoc).   Arginine (R)   Fmoc protected Arginine
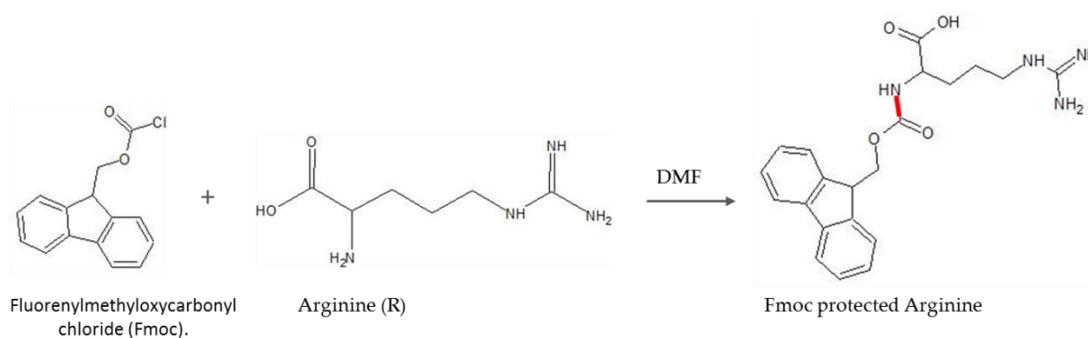
Reaction 1: Arginine undergoing Fmoc protection.

The N protection step is vital to a controlled synthesis and ensures that unwanted reactions are less likely to take place. In current practice, however, the amino acid residues that are used for peptide synthesis come in prepared vials in protected form. Not only are the nitrogens protected, but also any other reactive side chain groups of concern. As a result, the action of protecting no longer needs to be conducted in the lab; nevertheless a proper understanding of the process is still required to ensure correct automation of the instrument. Further control of the desired coupling is ensured by OH activation.

OH activation

OH activation is an additional step that ensures a controlled synthesis. It involves use of an activating agent, sometimes referred to as a coupling agent. Two of the most commonly used coupling reagents are: 2 - (1H - Benzotriazole - 1 - yl) - 1,1,3,3 - tetramethyluronium hexafluorophosphate and 2 - (6 - Chloro - 1H - benzotriazole - 1 - yl) - 1,1,3,3 - tetramethylaminium hexafluorophosphate (HCTU). In preparation for activation, the arginine is first subjected to N-methylmorpholine (NMM), an organic base that removes the acidic hydrogen from the carboxylic acid and, in this case, prepares it for a reaction with HCTU (Reaction 2). Just as the prepared amino acid vials come ready to use with N-protection, the vials also include the activating agent HCTU. The activating agent is used on the amino acid to be coupled which is itself Fmoc protected.

HCTU activating agent

+

Partially Fmoc protected Arginine (R)

DMF →

Fmoc protected, HCTU activated Arginine (R)

+

Byproducts
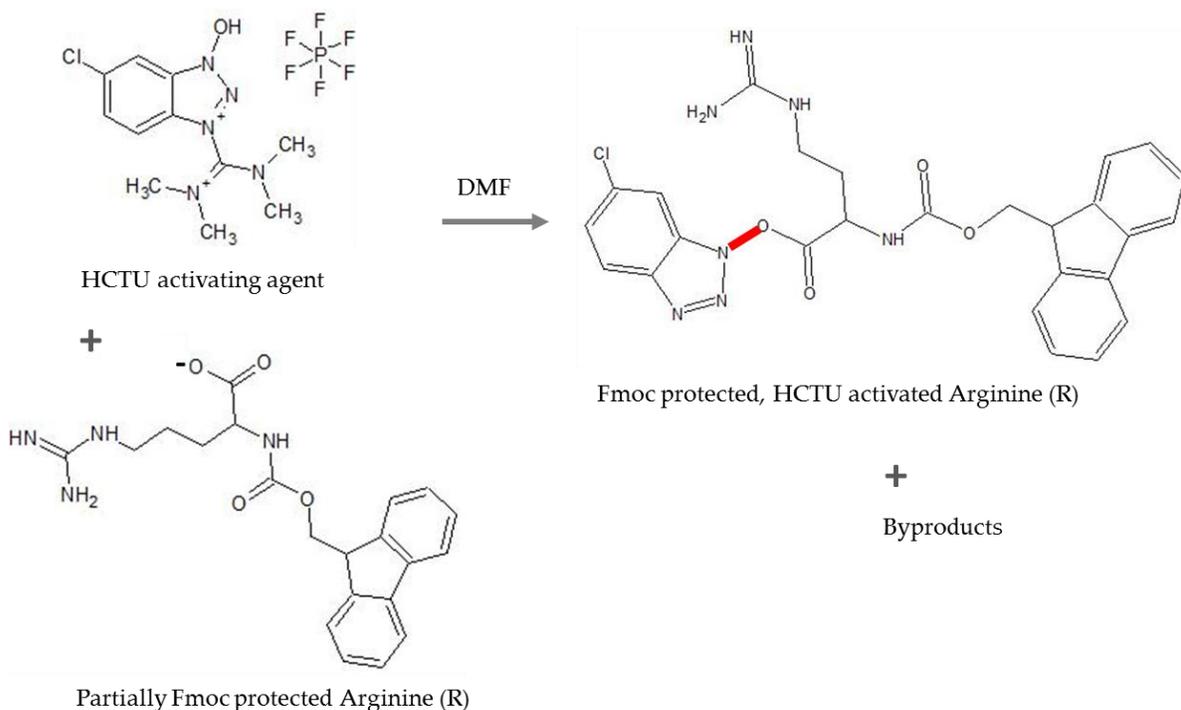
Reaction 2: Fmoc protected arginine amino acid that has been treated with the organic base NMM undergoing activation by the coupling agent HCTU.

Using the principles of 1) N protection and 2) OH activation, we can achieve a controlled synthesis by continuing with the steps of 3) Deprotection and 4) Coupling. The use of resin will be introduced to explain the addition of the first two arginine (R) residues to the growing indol peptide chain.

Peptide chain elongation

SPPS begins by coupling the first amino acid in the peptide series to a solid resin. There are many resin types available for use, for our purposes, rink amide resin was used which would yield an amidated C-terminus after resin cleavage. The addition of the first amino acid to the resin is similar to the coupling step of peptide

synthesis. Addition of protected and activated arginine forms a bond between the nitrogen of the rink amide resin and the carbon of the carboxylic acid (Reaction 3).

Rink amide resin

+

HCTU activated, FMOC protected
Arginine (R)

DMF

Rink amide resin coupled with Fmoc
protected arginine
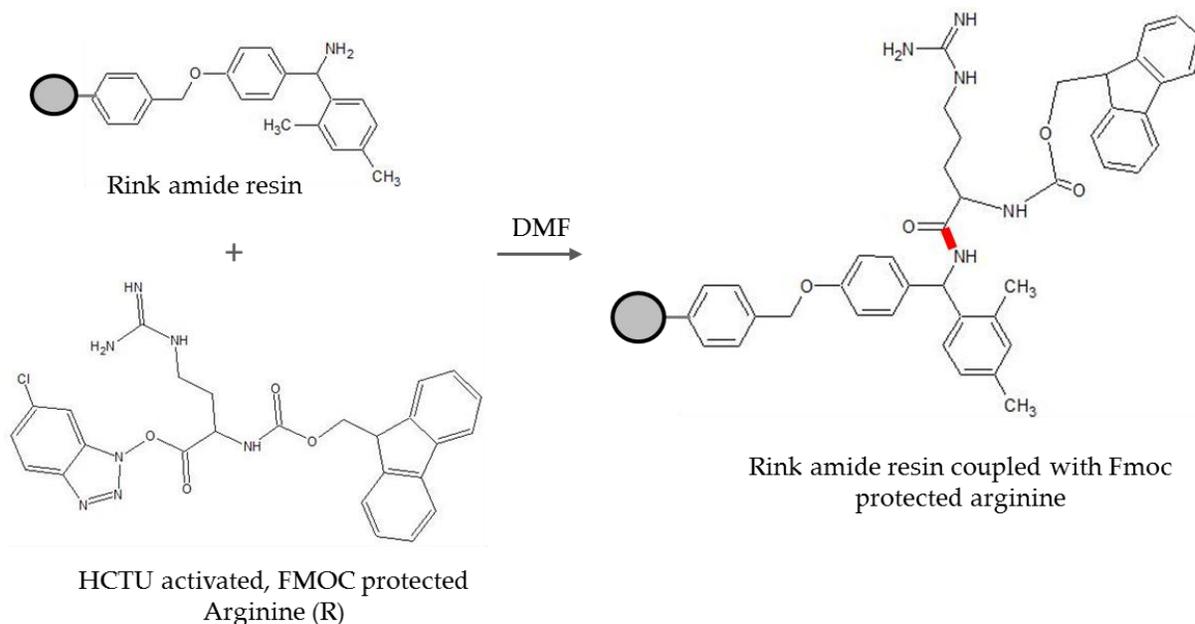
Reaction 3: Rink amide resin coupling with HCTU activated, Fmoc protected arginine (R).

Following coupling of arginine to the resin, we can proceed with chain elongation by deprotection and coupling to the next amino acid (Reaction 4). Deprotection is conducted on the amino acid that is already linked to the resin by use of piperidine which removes the Fmoc protecting group. Coupling will proceed in a very controlled manner because the arginine to be added to the reaction is itself Fmoc protected and HCTU activated. As such, the nucleophile and electrophile have been predetermined by use of appropriate protection and activation moieties.

Fmoc protected arginine coupled to rink amide resin

1) Deprotect with piperidine
2) Couple with amino acid in DMF

Byproducts

Fmoc protected, HCTU activated Arginine (R)
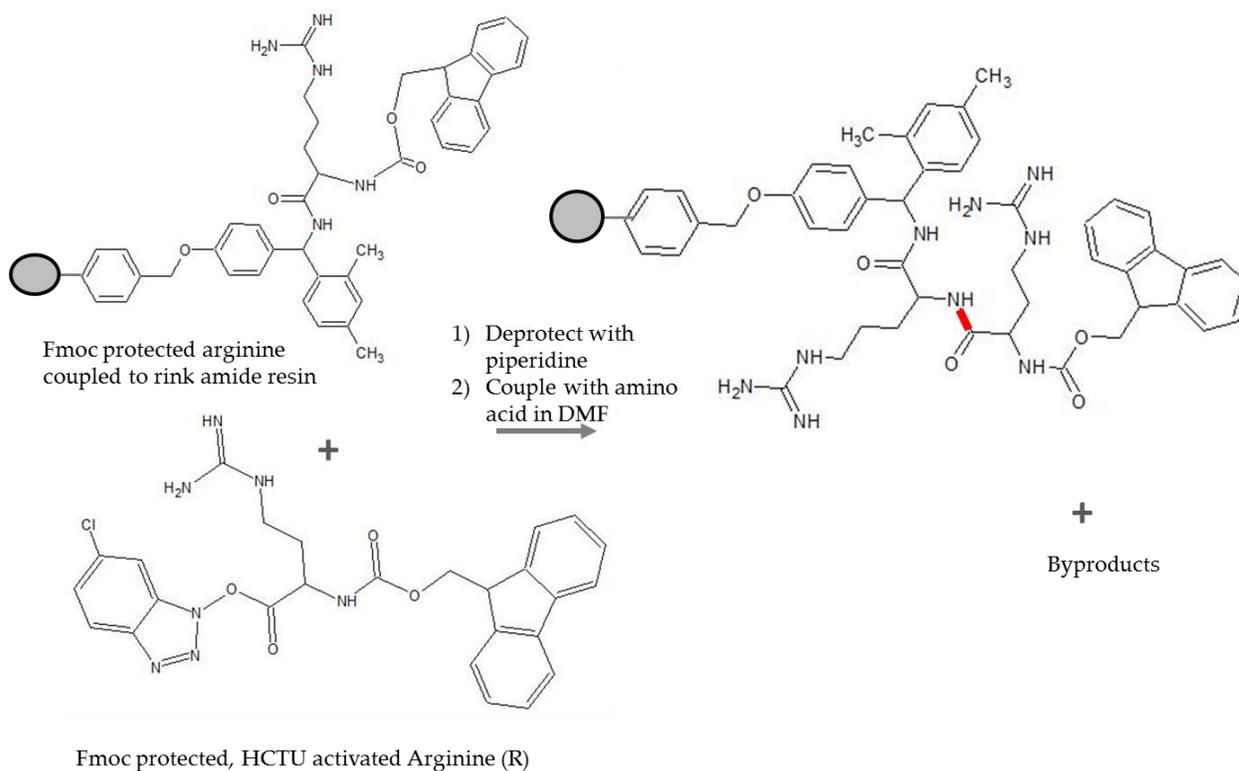
Reaction 4: Arginine amino acid coupling with Fmoc protected and HCTU activated Arginine. The result is two arginine residues in sequence attached to the rink amide resin. The second arginine of the sequence is still Fmoc protected.

To continue peptide chain growth, we would continue to deprotect the already coupled amino acid and couple to the next amino acid which would itself be Fmoc protected and HCTU activated. This series of steps is repeated until all 13 amino acids of the indol peptide have been coupled.

Experimental

Equipment and Reagents

The AMP indol (ILPWKWPWWPWRR-NH$_2$) was synthesized by SPPS using the Tribute®peptide synthesizer by Protein Technologies, Inc. The synthesis was conducted on a 0.1 mmol scale, and used amino acids in the standard five-fold excess. Prepared and sealed vials of Fmoc protected, HCTU containing amino acids were obtained from Protein Technologies. Vials in the 0.5 mmol scale were used primarily. When necessary, 1.5 mmol and 2.5 mmol vials were opened and divided into 0.5 mmol fractions.   The necessary quantities of reagents were determined by adding 50% to suggested volumes proposed by the instrument's "bottle calculations". Reagents were placed in designated Tribute® bottles (Table B1). Rink amide resin was obtained from Advanced Chemtech, Louisville, United States. Dimethylformamide (DMF) and piperidine were obtained from Sigma-Aldrich, Oakville, Ontario Canada.   A 20%v/v piperidine was prepared by mixing with DMF. The organic base NMM was made in 0.4 M by mixing with DMF.

Table B1: List of Tribute® bottles, their contents, volume and use during Indolicidin synthesis.

Bottle #	Reagent	Volume (mL)	Use
①, ②	Dimethylformamide (DMF)	600	Washing, swelling resin
③	20%v/v piperidine/DMF	150	Fmoc deprotection
④	0.4M N-methylmorpholine (NMM)/DMF	125	Base used during activation
⑤	Dichloromethane (DCM)	0	Cleaving, cleaning instrument

System Automation

Bottles were pressurized with N_2 to 9 psi and valves to 45 psi. The Tribute® was loaded with prepared amino acid vials in the C → N order. A single synthesis in one reaction vessel was programmed with the first amino acid to be added directly to the resin being assigned the "standard swell" program. The remaining 12 amino acid vials used the "standard coupling" program. Following completion of the amino acid coupling, a "standard deprotect and dry" program was used on the peptide chain to leave the terminal amino acid deprotected. The resulting peptide, still attached to the resin, was transferred to a small, well-sealed vial and placed in the freezer for storage until cleaving from the resin, purification and identification can be completed.

Achieving a purified indolicidin product

Although the Tribute® can cleave the peptide from the resin directly on the instrument using the dichloromethane (DCM) in bottle ⑤, the process is quite foul smelling and thus is preferably done in a fume hood with a cleavage mixture (82.5% trifluoroacetic acid (TFA); 5% thioanisole; 5% phenol; 5% water; 2.5% ethanedithiol)(1) . Cleaving takes approximately 8 h at room temperature (~23ºC) and yields the desired amidated C-terminus.

Purification and extraction remain before acquiring the final synthesized peptide. The TFA and DCM are removed by rotary evaporation and the peptide is then redissolved in water. Extraction into diethyl ether removes some impurities. Filtered samples are then injected into an HPLC and "the biggest peak" is manually collected. The HPLC is run with helium sparged filtered water (0.1% TFA)/HPLC-grade acetonitrile (0.05% TFA) gradient (1). In the past, lyophilization at Agriculture Canada was used to dry the final peptide. Verification of the final peptide sequence, to ensure that indolicidin was indeed synthesized, is best conducted by mass spectrometry.

References

1. Podorieszach AP, Huttunen-Hennelly H. The effects of tryptophan and hydrophobicity on the structure and bioactivity of novel indolicidin derivatives with promising pharmaceutical potential. Organic & biomolecular chemistry. 2010 04;8(7):1679-87.

2. Kerr JM, Banville SC, Zuckermann RN. Encoded combinatorial peptide libraries containing non-natural amino acids. J Am Chem Soc. 1993 03/01; 2014/02;115(6):2529-31.

3. Merrifield RB. Solid Phase Peptide Synthesis. I. The Synthesis of a Tetrapeptide. J Am Chem Soc. 1963 07/01; 2014/02;85(14):2149-54.

4. Bourgin D. Challenges in Industrial Production of Peptides. In press 2005.